UNIVERSITY OF CALIFORNIA,

IRVINE

Kinetics study of a solvent extraction system using a Nitsch Cell

THESIS

MASTER OF SCIENCE

in Chemical and Biochemical Engineering

by

Alba Bosch Font

Thesis Committee:

Professor Mikael Nilsson, Chair

Professor Elizabeth Read

Professor Diego Rosso

2018

TABLE OF CONTENTS

LIST OF FIGURES

LIST OF TABLES

ACKNOWLEDGEMENTS

I would like to express my sincerest gratitude to Mr. Pete Balsells and Professor Roger Rangel for giving me the invaluable opportunity to pursue my Master of Science degree at UC Irvine. This thesis and my experience in California would never have been possible without the support from the Balsells Fellowship.

I would also like to thank Professor Mikael Nilsson, Professor Elizabeth Read and Professor Diego Rosso for serving on my thesis committee and taking the time to read and review this work. I would like to extend my gratitude to my advisor and chair of the committee Prof. Nilsson for welcoming me into the Nuclear Lab and for all his guidance and support during the progress of this project.

Furthermore, I would like to thank all the members of the Nuclear Lab for helping me whenever I have needed it. Especially, I would like to thank Tro Babikian for all what I have learned from him, for his support and guidance, and for sharing with me the challenge of making the Nitsch Cell possible. I would also like to acknowledge the help received from Jonathan Wallick at the UCI TRIGA nuclear reactor and for his help in improving the Cell. In addition, I would like to thank Dr. Nitsch and Dr. Geist from the Institut für Nukleare Entsorgungstechnik (INE) for sharing with us their Nitsch Cell design.

Finally, I would also like to mention my deepest gratitude towards the Balsells Fellows and my other friends I have met in Irvine: thank you for sharing this journey with me and making this an experience that I will always take with me. Last but not least, my most special gratitude goes to my family for his unconditional support and understanding. This enriching experience would never have been possible without the education and the values that you have always fight to provide me with, and for this, I will never be able to thank you enough.

ABSTRACT OF THE THESIS

Kinetics study of a solvent extraction system using a Nitsch Cell

by

Alba Bosch Font

Master of Science in Chemical and Biochemical Engineering

University of California, Irvine, 2018

Professor Mikael Nilsson, Chair

Solvent extraction is one of the most used techniques for Used Nuclear Fuel (UNF) reprocessing and Rare Earth Elements (REE) separation. Therefore, understanding the extraction kinetics is a key aspect for enabling further advancements in design and operation of future units for sustainable nuclear energy generation. For this project, a constant interfacial area stirred cell, a so called Nitsch Cell, was built, tested and optimized for studies on solvent extraction kinetics. In addition, the cell was utilized for the investigation of the extraction of trivalent dysprosium (III) into the extractant 2-ethylhexylphosphonic acid mono-2-ethylhexyl ester (or also known as HEHEHP) dissolved in Isopar L. The extraction mechanism was defined, as well as the rate controlling step and the forward reaction rate expression. The experimental results indicated that the extraction rate was not independent of the interfacial area. Furthermore, the extraction rate showed a linear increase with the stirring speed from 150 rpm to 400 rpm, indicating that the kinetic regime was diffusion-limited in that range. Decreasing the extractant concentration 4 times resulted in a shift of the observed kinetic constants to approximately 10 times lower, but the extraction regime did not change as the chemical reaction rate remained fast compared with the diffusion rate. The initial dysprosium fluxes and their dependency on the stirring speed were also analyzed and the individual mass transfer coefficients of each hydrodynamic condition were provided from this study.

1. INTRODUCTION

It is likely that in the near future we will experience an energy crisis as worldwide energy demand, especially electricity, is expected to increase by 28 percent by 2040 according to the International Energy Outlook 2017 Report. [1] Therefore, an efficient, secure, clean, and competitively priced supply of energy is vital for sustainable development. While a variety of renewable energy sources such solar, modern biomass, wind, or hydro will play a key role in reducing fossil-fuel dependence, they are still not efficient nor reliable enough by themselves to satisfy the world energy demand.[2]

Nuclear and hydroelectric power are the only proven technologies for efficiently generating base-load electricity that is carbon-free, which helps mitigate air pollution and therefore the threat of climate change. In addition, nuclear energy is efficiently produced in large scale and, as opposed to some renewable energies such as solar, wind and hydro, does not depend on the location of generation. Another advantage is its high-energy density, which allows the release of several thousand times more energy per mass of fuel than fossil fuels. Consequently, the amount of fuel required in nuclear plants is much smaller than other types of power plants. [2][3]

Nevertheless, to achieve the full potential that this energy source offers, there is a critical aspect that needs to be addressed: the dangerous radioactive waste produced in the nuclear fuel cycle, which lasts for hundreds of thousands of years. Significant improvements have been achieved to make nuclear reactors less vulnerable to accidents, but the significant reduction of nuclear waste generated during energy production is the decisive aspect to making this energy a powerful solution for the energetic crisis the world is currently and will continue to face.

Specifically, to contribute to this goal, effort is focused on the optimization of the Annular Centrifugal Contactor (ACC). ACC's have been used for solvent extraction processes since their development in the

1970s as part of nuclear fuel cycle research and development at U.S. Department of Energy facilities. [4] Solvent extraction or liquid-liquid extraction is a separation method that can enable greater utilization of the uranium resources as well as provide waste management benefits from removing long-lived actinides like plutonium, neptunium, americium and curium from the rest of the used fuel constituents. This process of reprocessing spent nuclear fuel not only reduces the amount of nuclear waste but it also minimizes the long term radioactivity of used nuclear fuel and enables the preservation of natural resources. [5]

Solvent extraction is also used for the separation of Rare Earth Elements (REE), which are the fifteen lanthanides, as well as scandium and yttrium, from different streams. Despite the name, rare earth elements are quite abundant in the earth's crust, but they tend to occur together in nature and are difficult to separate from one another. The high interest in these elements lies in their magnetic and optical properties, which make them indispensable in green technology such as wind turbines and hybrid electric vehicles. A projected threat to supply has prompted researchers to improve the separation methods to not only extract virgin REE from its minerals but also from other sources of REEs such as industrial scrap and waste electrical electronic equipment (WEEE). [6]

The Annular Centrifugal Contactor's high extraction performance, compact size and short processing time are some of its numerous advantages that make it a very efficient and safe technology for solvent extractions to process radioactive streams. Some of the work in progress in the Nilsson Lab at UCI investigates the mass transfer between the distinct phases in solvent extractions occurring in a miniature 1.2 cm rotor diameter contactor. In order to predict the magnitude of mass transfer occurring during the extraction, the interfacial area of the phases in the mixing zone must be known, among many other factors.[7] However, the contact area of the different phases in the mixing zone is not evident nor simple to measure since the flow characteristics in ACCs are very complicated and highly dependent on both geometrical and operational parameters [8]. The kinetics of liquid-liquid extraction of metal species can be a function of both the chemical reactions taking place in the system and the rates of diffusion of the

species present in the two phases. Since the contact area of the two phases is not evident in an ACC, it is crucial to find methods to study the kinetics from the chemical reaction involved in the solvent extraction discriminating any diffusional effects. In addition, the rate of solvent extraction can be characterized by the slow step of the overall reaction mechanism, which can occur either in the bulk (homogeneous reactions) or at the liquid-liquid interface or in a thin volume region very close to it. Although a relatively large number of sophisticated techniques are available for studying chemical reactions at solid-fluid interfaces, very few tools have been developed to investigate chemical changes occurring at liquid-liquid interfaces. For this reason, the knowledge of interfacial reactions is still limited and based on indirect evidence and speculations. [9]

In this work, a constant interfacial area stirred cell was constructed and used to make a kinetic study of an extraction system. The stirred cell used is called a Nitsch Cell and its functionality allows the liquid-liquid extraction between two immiscible liquids to occur while leaving the contact area between the two liquids undisturbed. [10] Thanks to the Nitsch Cell design, the two bulk phases can be completely stirred allowing turbulent mixing in the bulk of liquids while maintaining a constant and known interfacial area. Ideally, the effect of diffusion can be minimized by increasing the mixing of the bulk phases, which reduces the thickness of the laminar zone, where the interface between the two liquids exists. This allows for studying the extraction process at different hydrodynamic conditions to determine the rate-controlling step: the diffusion of species through the interfacial stagnant layers or the chemical reaction occurring when the species reach at the interface. In addition, since the interphase area is constant in the cell, the kinetic information obtained in a Nitsch Cell can be compared to that from the same extraction occurring in an ACC. Then, a back calculation of the chemical reaction rate can be used to calculate the contact area of the two phases interface in the ACC, as done in the study carried out by El-Hefny Hot in 2006. [10]

Thus, the objective of this project was to build in-house, at the machine shop of UCI, a constant interface stirred cell with the Nitsch Cell design provided by the Institut für Nukleare Entsorgungstechnik (INE). An important part of the work done was to improve the cell layout and define the appropriate set up and experimental procedure to use the cell. Then, the Nitsch Cell was used to start developing a kinetic study of the extraction of lanthanides into an organic phase containing a widely used extractant. Specifically, the lanthanide used was dysprosium (III) contained in nitric acid, and the organic phase was composed of Isopar L and the extractant 2-ethylhexylphosphonic acid mono-2-ethylhexyl ester (HEHEHP).

The kinetic information from solvent extraction systems is a crucial aspect for enabling further advancements in design and operation of future units to make the Nuclear Energy more sustainable and efficient. This will determine the success of future advanced fuel reprocessing facilities, as well as many other chemical processes, such as in pharmaceutical productions and oil-water separations. [4]

2. BACKGROUND

2.1. Liquid – liquid extraction

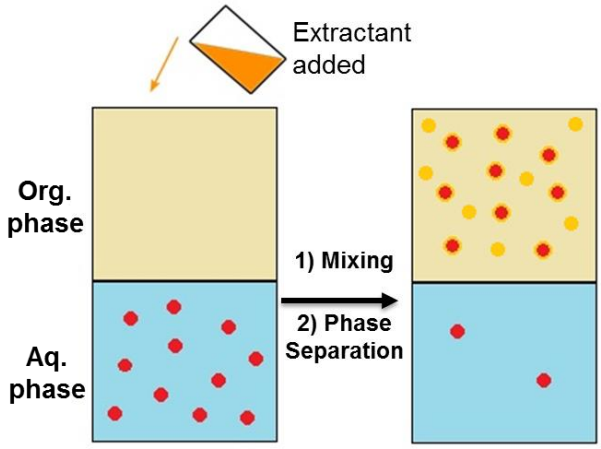

Figure 1. Representation of a batch liquid-liquid extraction of a compound (red) from an aqueous phase into an organic phase containing an extractant substance (orange).

Liquid-liquid extraction (also known as solvent extraction) was initially utilized, on a large scale, in the petroleum industry beginning in the 1930s. Since then, it has been an important procedure utilized in numerous applications including the pharmaceutical, petroleum, metallurgical and nuclear industries. [11] Liquid-liquid extraction is a technique to separate compounds from one liquid into another utilizing an unequal distribution of the components between the two liquid phases which are immiscible. This process consists of mixing the two immiscible phases allowing for the selective transfer of one or more solutes from one phase to the other and, afterwards, allowing the two phases to separate (see Figure 1). Typically, the phase containing the compound to be extracted is an aqueous solution, and the other phase is an organic solvent containing an extractant substance which has a high affinity for the specific species to be separated from the former phase. The two immiscible liquids have a density difference which enables a rapid separation of the phases after being mixed together. [11][12] The distribution ratio (D) of the solute, also known as the distribution coefficient or distribution factor, is defined as the total analytical

concentration of the substance in the organic phase to its total analytical concentration in the aqueous phase, usually measured at equilibrium. If the target to be extracted is the solute A, the distribution ratio at time t is defined as in **Equation 1** where the brackets indicate concentration at time t in each phase, "org" indicates organic phase and "aq" indicates aqueous phase:

$$\mathbf{D(t)} = \frac{\mathbf{[A]^t_{org}}}{\mathbf{[A]^t_{aq}}} \qquad \text{Equation 1}$$

In industrial applications, the extraction result is often expressed as an extraction percentage (%E), as in **Equation 2**:

$$\%\boldsymbol{E} = \mathbf{100}\frac{\boldsymbol{D}}{\mathbf{1}+\boldsymbol{D}} \qquad \text{Equation 2}$$

The extraction process is reversible by contacting the organic solvent loaded with the previously extracted solute with another immiscible phase that has a higher affinity for the solute than the organic phase. This reverse extraction is called stripping or back-extraction. [10]

The solvent extraction procedure can be realized by a batch equilibrium contact of the two phases, but one of the main advantages of the separation process is that it can be realized in a continuous mode, which allows for a high separation factor while operating at high processing rates. [11]

2.2. Extraction equipment

There are three basic types of equipment used in industrial-scale nuclear solvent extraction processes: mixer-settlers, columns and annular centrifugal contactors.

The mixed settlers are comprised of two sections: the mixing section, where the two immiscible liquids are mixed using an impeller, and the settling section, where the two phases separate under gravity force due to density differences (see Figure 2). Mixer-settlers are useful for slow kinetic

processes because they provide long residence times and the solutions are easily separated by gravity. They require a large facility, but do not require much headspace. [11] [13]

There are two types of columns utilized in industry for solvent extraction, through which the two phases involved flow in a counter current mode: packed columns and pulse columns with plates or trays. Packed columns contain pieces of packing material that creates a tortuous path that ensures constant contact as the two solutions flow through the equipment. They offer a simple operation as there are no moving parts, but are not very efficient. The number of stages is determined by the height of the column, so a system that requires several stages to achieve the desired separation implies a very tall column. The pulsed columns allow for a height reduction as they have perforated plates that generate droplets of the two phases involved in the extraction. Typically, pressurized air is injected into a pulse leg that pushes the liquids in the column up and down. This pulsing action reduces droplet size of the dispersed phases, maximizing their contact area and improving mass transfer. A settling chamber exists at the end of the column where the organic phase is completely separated from the aqueous droplets that might have reached the chamber (see Figure 3). Pulsing devices and pulse speed controllers are required, and periodic maintenance is required only for the pulsing equipment. Pulse columns are used when a process requires intermediate residence times, as residence time is easily varied by adjusting flowrate. They do not need much space to be installed but do require significant headspace (typically 40-50 feet). [11] [13]

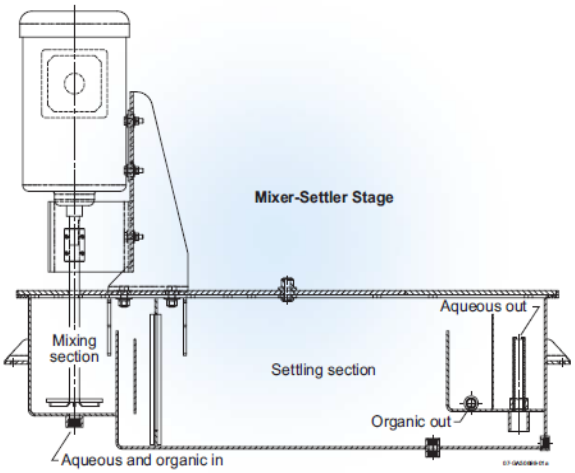

Figure 2. Mixer-Settler. [11]

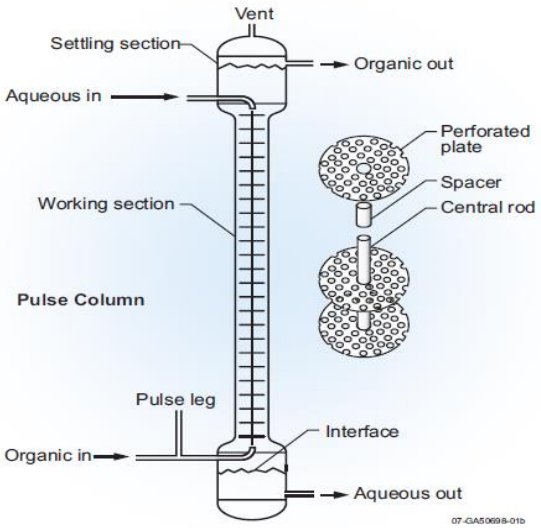

Figure 3. Pulse Column with perforated plates. [11]

The third extraction equipment is the Annular Centrifugal Contactor (ACC), which has relevant advantage compared to mixers-settlers and pulsed columns: compactness, efficiency and minimal degradation of the organic phase due to a rapid phase separation under high centrifugal forces. In the ACC, the two immiscible liquids enter a narrow annular gap between the stationary outer housing and the rotating outer surface of the spinning rotor, where the mixing occurs. Below the rotor, there are stationary vanes which serve to break the rotation of the fluids being mixed and direct the dispersion towards the interior of the rotor. The high-speed rotation of the rotor separates the two immiscible phases due to centrifugal forces, pushing the heavy phase towards the exterior. The rotation also serves as a pump which directs the two phases upwards, where they become fully separated and split off: the heavy phase leaves the ACC through an exit at the outer wall of the rotor and the light phase leaves through the exit at the center of the rotor. [4] In this way, the contactor performs as a mixer, centrifuge and pump using a compact single moving part. (See Figure 4)

Great efforts are being made to improve this technology, as it is a crucial equipment for the future of used nuclear fuel reprocessing. Some research focuses on the hydrodynamics occurring during the mixing step: the contact area of the different phases in the mixing zone is not evident nor simple to measure since the flow characteristics in ACCs are very complicated and highly dependent on both geometrical and operational parameters [8]. The kinetics of liquid-liquid extraction of metal species can be a function of both the chemical reactions taking place in the system and the rates of diffusion of the species present in the two phases, which is highly dependent on the interfacial surface. Since the contact area of the two phases reacting in the mixing zone of an ACC is not evident, it is challenging to make complete kinetic studies with these reactors. In addition, in order to predict the magnitude of mass transfer occurring during the extraction it is required to know the interfacial area of the phases in the mixing zone, among many other factors. For these reasons, another kind of equipment is required to study the kinetics of solvent extractions discriminating between the diffusional effects and the chemical reactions. This is possible by using a constant interfacial stirred cell, in which the effect of diffusion can be minimized by increasing the mixing speed of the bulk phases. In addition, since the interphase area is constant in these cells, the kinetic information obtained in a highly diffused experiment can be compared to that from the same extraction occurring in an ACC. Then, a back calculation of the chemical reaction rate can be used to calculate the contact area of the two phases interface in the ACC, as done in the study carried out by El-Hefny Hot in 2006. [10] An extended explanation about the kinetics in a constant interfacial area stirred cell can be found in the following section, **Constant interfacial area stirred cell**.

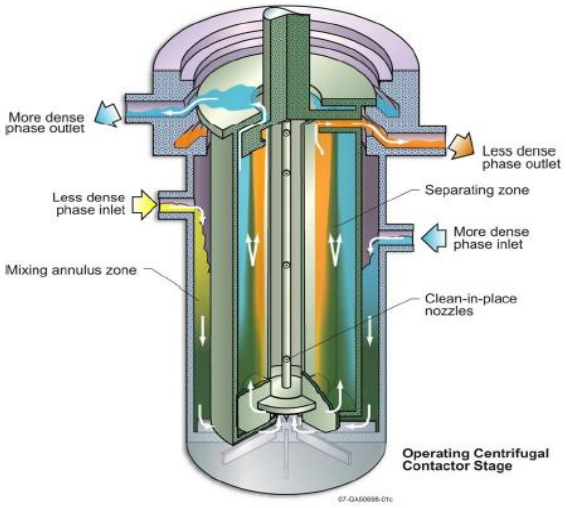

Figure 4. Cutaway view of an operating Annular Centrifugal Contactor. [11]

3. LIQUID-LIQUID EXTRACTION KINETICS

The kinetics of liquid-liquid extraction of metal species from aqueous solutions can be a function of both the chemical reactions taking place in the system and the rates of diffusion of the species present in the two phases. [14][15] The rate of solvent extraction can be characterized by the slow step of the overall reaction mechanism, which can occur either in the bulk (homogeneous reactions) or at the liquid-liquid interface or in a thin volume region very close to it. [9] In addition, diffusion processes can also be rate determining, as the chemical species have to be transferred from one phase to another for the reaction to occur, and the transport of material from the bulk to or from the interface can be significantly slower than the actual reaction. Depending on the relative velocity of the transport of material in extraction of metal species compared to the rate of the chemical reactions taking place in the system, we can define 3 different kinetic regimes: chemical reaction-limited, diffusion-limited and mixed regime. [10]

3.1. Extraction Regimes

- **Diffusion-limited regime:**

The “diffusion-limited regime” occurs if the chemical reactions are sufficiently fast; the extraction rate is determined only by the diffusion processes occurring in the laminar diffusion films existing in the interface of the two liquids. In this case, the kinetics of solvent extraction can be treated in terms of diffusional theories as the mass transfer velocity dominates compared to the chemical reaction velocity, which can be considered instantaneous. This situation can be found either when the transported species have very large diffusion coefficients or when the diffusion films have a relevant thickness. [14]

- **Chemical reaction-limited regime:**

When the diffusional processes can be considered practically instantaneous with respect to the chemical reactions, the extraction process is considered entirely chemically controlled and the system is said to be in a "kinetic regime". [14]

- **Mixed regime:**

However, in practice it is often difficult to find pure diffusional regimes and pure kinetic regimes, as they are not completely unambiguous when applied to experimental data. In these cases, to fully describe the kinetics of extraction it is necessary to simultaneously solve the equations of diffusion and the equations of chemical kinetics. A mixed regime can therefore be described as a case of mass transfer with slow chemical reactions, where the rates of diffusion and of the chemical reactions can never be neglected with respect to each other. This unambiguous identification of regime introduces both experimental and theoretical difficulties: the former difficulties are due to the fact that a large set of different experimental information obtained in self-consistent conditions is needed, and the latter difficulties are due to the fact that the solution to differential equations have no analytical solutions and have boundary conditions that need to be determined experimentally, unless the introduction of simplifying assumptions is demonstrated as legitimate. [14]

3.2. Technique to determine the kinetic regime

The experimental identification of the extraction regime controlling a specific system can be done by studying the extraction rate dependency on the diffusion rate of species through the laminar layer conforming the interface between the two phases of the liquid-liquid extraction. However, this is in general challenging due to the fact that sometimes the rates may show the same dependence on either hydrodynamic and concentration parameters, even though the process responsible for the rate of extraction is different, i.e. diffusion or chemical reaction. In these cases, it is necessary to supplement the investigations of hydrodynamics and concentration of chemical species with other information concerning the biphasic system such as the interfacial tension, the composition of species existing in the solutions, or the solubility of the extractant in aqueous phase.

3.2.1. Constant interfacial area stirred cell

The most useful method for identifying the extraction regime is a kinetic study using a constant interfacial area stirred cell, often called a Lewis-type cell, in which the liquid-liquid extraction can occur while the contact area between the two phases is kept constant and stable.

In a stirred cell, the light and heavy phases are separated while two blades (one in each bulk) generate a turbulence that allows individual mixing of each phase without disturbing the interface between the two immiscible liquids. [10] If the bulks are efficiently stirred, the diffusional effects are limited to a zone in the proximity of the interface. Therefore, the interface consists of 3 parts: two stationary layers (one on the aqueous side and one on the organic side) and the zone where they contact each other (see Figure 5). The thickness of these diffusion films is a function of the hydrodynamic conditions occurring inside the system: the faster a bulk is stirred, the thinner the layer of that phase is and, as a consequence, the shorter the path for the species to reach the interface and react with other reagents. [14]

This technology is used to determine the initial rate of extraction as a function of the stirring speed of the phases at constant interfacial area, as it allows both the knowledge of the contact area between the two phases and the variance of the stirring rate of the bulks. At low stirring speeds, the thickness of the stagnant interfacial layers from the interface (see Figure 5) is so large that the process of diffusion of the metal species to the interface is very slow and dominates over the extraction rate. At high enough stirring speeds, if the interface can be maintained undisrupted, the thickness of the stagnant layer will

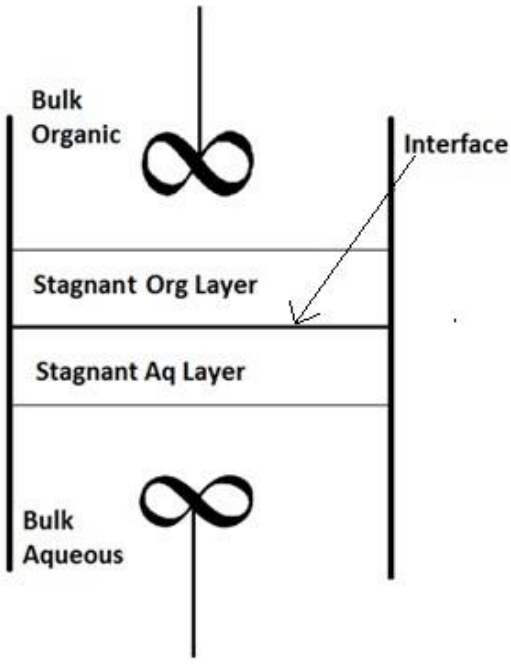

Figure 5. Schematic of a Constant Interfacial Area Stirred Cell.

approach zero, reducing the diffusional effects and making the chemical reaction rate more relevant to the extraction rate.

In addition, by evaluating how the rate varies with the interfacial area while the hydrodynamic conditions are kept constant, it is possible to distinguish between a kinetic regime controlled by interfacial or by bulk chemical reactions.

When the initial rate of metal extraction $r_o = \frac{-dC}{dt}$ at time approaching zero (C being the molar concentration) is measured in the stirred cells as a function of stirring speed of the aqueous phase (n_{aq}), a plot of the initial rate versus the stirring speed (r_o vs. n_{aq}) is always characterized at the beginning by a linear behavior, which indicates the extraction rate is only diffusion controlled. [10] [14] This can be explained by the fact that, even if a slow heterogeneous or homogeneous chemical reaction occurs in the system, at low stirring rates the thickness of the stagnant interfacial film is always so large that the process of diffusion preceding the arrival of the metal species to the interface is always the slowest one. Because the relationship between the mass-transfer coefficients and the rate of stirring is linear, the relationship between r_o and n_{aq} will also be linear (see Figure 6). Since heat is transported through diffusion-like processes, in these cases where the rate of extraction is only controlled by diffusion, the same linear dependence occurs between of the heat-transfer coefficient and n_{aq}.

When a slow heterogeneous or homogeneous chemical reaction starts to become competitive with the diffusional processes in controlling the rate of extraction, the progressive increase of the stirring rate will no longer cause proportional increase in r_o, up to a point where a further decrease of thickness of the stagnant films will have no influence at all on the overall velocity of the extraction process. Therefore, the reaction rate will be independent of the stirring rate, and the plot of r_o vs. n_{aq} will show a plateau after the previously described linear portion (see Figure 7). It can be concluded that the system described in Figure

7 has an extraction zone controlled by diffusion from 0 to 100 rpm, and by chemical reaction from 100 rpm to higher stirring speeds.

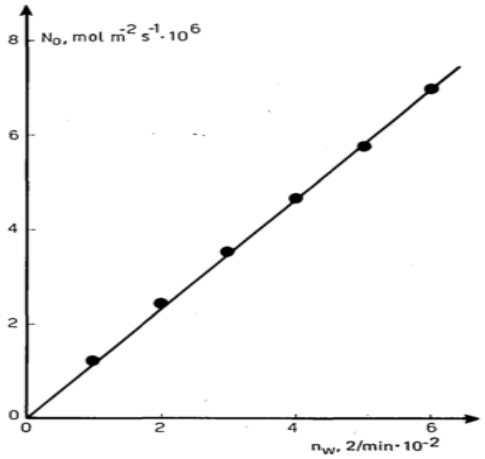

Figure 6. Stirring speed influence in the aqueous phase (n_{aq}) on the initial interfacial flux (N_o) for the transfer of Zn^{2+} from an aqueous phase into a dithizone solution in CCl4. [14]

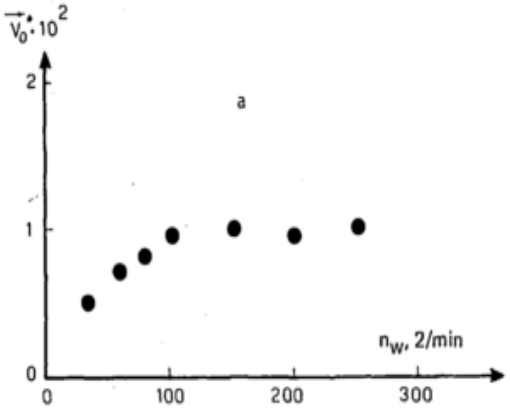

Figure 7. Influence of the stirring speed in the aqueous phase (naq) on the initial forward mass-transfer rate (ro) of Fe+3 between aqueous HCl solutions and toluene solutions of trilaurylammonium chloride. [14]

However, plateau regions can also be generated by other phenomena and it is still possible that, even though the experiment has not showed dependence between extraction rate and stirring speed, the rate of extraction is still diffusion controlled or, at least not fully kinetically controlled. For example, a physical reason of independence between r_o and n_{aq} can derive from the "slip effect", during which the agitators can lose efficiency at high speeds and the thickness of the stagnant diffusion films is unaffected by the increased rotation of the blades. [14] Another reason for this phenomenon is a chemical one. If there exist some side-reaction products that are coordinately unsaturated and then polymerize at the interface, forming films, these films can present a high diffusional resistance that might cancel the effects of increasing n_{aq}. These films have been reported to exist during the extraction of heavy metals, such as Zr or Ti, by alkylphosphoric acids. [10] [14] A third example for the independence of r_o and n_{aq} occurs when the biphasic system is characterized by very intensive interfacial instabilities of the Marangoni type. The Marangoni effect (also called the Gibbs–Marangoni effect) is the mass transfer along

an interface between two fluids due to surface tension gradient. Instabilities of these type can produce a degree of local mixing, and therefore transfer can occur also in total absence of bulk agitation.[16] In this case, a plateau might occur from $n_{aq} = 0$ to some moderate value, before the region where r_o starts to be proportional to n_{aq}. In conclusion, only when these plateau-simulating effects can be excluded, can the plateau region be reliably attributed to an extraction rate controlled by chemical reactions.

3.2.2. The interface

The chemical reactions during an extraction in a stirred cell can occur either in the bulk phases or at the interface. The distinction between the two types of reactions can be performed by studying how the initial rate of extraction (r_o) varies both with the interfacial area and the volume of the phase from which the metal species is extracted. If the initial rate is independent of both the volume and the interfacial area, it can be concluded that the slow chemical reactions occur in the bulk phase. Otherwise, they must occur at interface of the system. [10] [14]

The interfacial area coincides with the geometrical horizontal section of the cell where the two phases are permanently separated, and it must be kept always constant when the degree of stirring of the two phases is varied over the widest possible range. The cell built for this project has a distinctive design to maximize the stirring speed range at which the interface is not disrupted. A cylinder (guiding tube) surrounds each of the two stirring blades, allowing for higher stirring speeds and still providing homogeneous mixing of the entire bulk of a phase (see section **Nitsch Cell Characterization**).

The physical properties (density, viscosity, etc) in the interface can be different from those in the bulk and generally they are unknown. Extracting reagents are characterized by both a hydrophilic and hydrophobic nature. The hydrophilic group normally interacts with the metal, and the hydrophobic group is what allows solubility in the water-immiscible organic diluent. For this reason, the zone that the extracting reagents prefer to operate in is the interface, where their free energy of solution is minimized. Due to this

adsorption, extracting agents often exhibit surface active properties and the interfacial concentration can be larger than that of the reagent in the organic bulk. This can make it more favorable for the reaction to occur at the interface, which can show an interfacial resistance and can be sufficiently slow, affecting the crossing of the interface by metal species. Most solvent extraction reagents will exhibit interfacial activity at an oil-water interface, which is the system used in this thesis.

3.2.3. Nitsch Cell Characterization

Several different versions of Constant Interfacial Area Stirred Cells, also known as Lewis Cells, have been reported in the literature. [17][18][19][20][21] The main differences between them lie in the shape and dimensions of the stirrers, which drive the forced convection, and in the presence or absence of internal baffles, which modify the internal forced convection. The stirred cell built at the University of California, Irvine uses the design from the Nitsch Cell built at the Institu für Nukleare Entsorgungstechnik (INE) (see Figure 8). Nevertheless, the dimensions and materials of some parts have been modified for convenience during the building process and for solving some problems that appeared during the start-up of the system

Figure 8. Institut für Nukleare Entsorgungstechnik (INE) Nitsch Cell design.

Figure 9. Nitsch Cell built at the University of California Irvine.

(see Figure 9). The main metal structure, the shafts, the stirrers and the legs of the cell were made of stainless steel 316 and manufactured at the UC Irvine Research Machine Shop. The manufacturing of the two concentric glass cylinders that form the cell's walls was outsourced to an external glass manufacturer, and the rest of the parts were bought from external suppliers.

- **Stirring Speed Range**

In order to maximize the range of variation of the stirring speed of the phases without rippling or disturbing the interphase, the Nitsch Cell cell contains cylinders (guiding tubes) that surround the stirrers. These shields limit the maximum size of the eddies and transform most of the translational kinetic energy of the liquids into turbulent energy. INE Nitsch Cell's design used glass small cylinders for this purpose (see Figure 8). However, it was not possible to use glass guiding tubes for the cell built for this study since the tolerances were to big due to manufacturing limitations: for all the guiding tubes built, the glass was either too thin, such that the cylinder would be loose in the cell, or the glass was so thick that the piece would crack when assembled in the cell around the stirrer. The first attempt to fix the problem was to switch to polymethyl methacrylate acrylic (PMMA) (see Figure 10 (A)) , also known as acrylic glass material, the manufacturing of which is more precise and which offers the same resistance to the chemicals used as glass does. [22] However, after facing some problems of consistency among the experiments performed in the cell, the cleaning procedure had to be changed to use a stronger acid (see section **Nitsch Cell Characterization, Cleaning and Maintenance),** which degraded the PMMA cylinders. For this reason, the material was

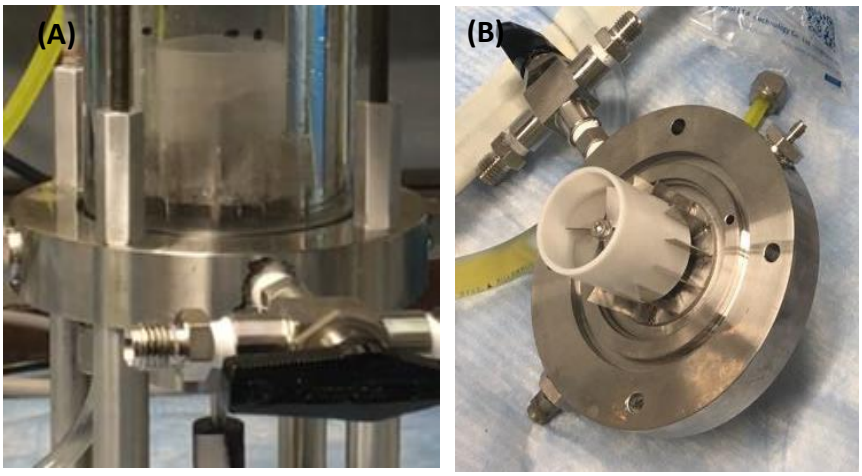

Figure 10. (A) PMMA guide tube. (B) Teflon guide tube.

changed to Teflon, which on the one hand is not transparent, but is resistant to strong acids even during 30 days of constant exposure (see Figure 10 (B)). [22]

- **Motors**

The system of motors that was chosen for the cell built for this project allows the changing of the revolution number of the stirrers in the two phases independently. In this way, the stirring speed of one of the phases, the aqueous or the organic, can be kept constant while the other is varied in order to identify the effects of reducing the thickness laminar layer in that specific medium. In addition, the ability of stirring the two bulks at different speeds allows the influence of the density and viscosity of the two phases to be taken into account, and the liquids can be agitated at the same Reynolds numbers.

For the first set of experiments, which showed inconsistent data among experiments done at the same conditions, two basic motors were used to stir the aqueous and organic bulk. These motors had to be calibrated before each experiment plotting the rotation speed (rpm) versus the voltage supplied. However, while the experiment was running, the motors overheated and the rotation speed decreased significantly. The rpm was also affected by changes in liquid volume inside the cell, which happened when some of the liquid leaked out or after sampling. For this reason, the initial stirring system was replaced for a more robust one. This new system consisted of two motors connected to two independent drives programmed to automatically modify the voltage input of the motors in order to maintain a constant stirring

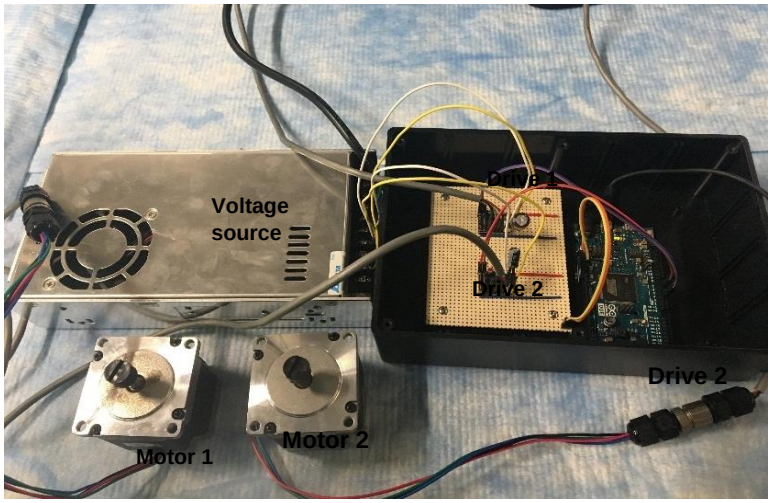

Figure 11. System of motors to maintain a constant stirring speed.

speed (see Figure 11). For both the initial and the second system, a handheld digital laser photo-tachometer was used to check the real rotation speed of the motors.

- **Filling the cell**

It is important to set the interface at exactly at the same position for every experiment, right in the middle of the two guide tubes, because the interface level has an influence on the hydrodynamics (see Figure 13). In Figure 13, the inlet for the two bulk liquids is indicated. The aqueous phase (heavy phase) was introduced, using a syringe, from the bottom up to the points indicating the phase level (see interface label in Figure 13). The syringe was weighed to make sure the correct volume of liquid had been introduced. Then, the organic liquid was injected from the upper inlet with another syringe until the phase reached the top of the cell.

- **Temperature bath**

The Nitsch Cell consists of two concentric glass cylinders. The inner cylinder is where the solvent extraction takes place, and the outer one is connected to a water bath which allows the continuous circulation of water at a specific temperature through the annular gap surrounding the inner cylinder. This system not only eliminates any effects due to room temperature fluctuations, but also allows for kinetic studies at a wide range of temperatures.

- **Sampling**

The upper flange of the cell (see Figure 12) has 3 sampling points: two for online monitoring of the concentration of the species being extracted as a function of time (bypass connectors) and one for manual discrete sampling (sample port). For continuous monitoring, an external bypass loop can be connected to either the upper and/or lower flange (to sample from both phases of the extraction system) using a 1/16" loop connector on the respective flange. The online analysis can be done by either radiometric, electrochemical or optical techniques. The advantages that come from continuous monitoring are that the

volume variations caused by volume samplings are eliminated, and it is experimentally convenient as the sampling procedure is faster and automated.

The sample port on the upper flange allows for discrete sampling by introducing a syringe with a needle that reaches the upper bulk of liquid. By using a sufficiently long needle, samples can also be drawn from the heavier phase. However, for the experiments done in this project, the discrete sampling of the heavier phase was done through one of the bypass connector points of the lower flange. The port was capped with a septum to prevent from leaks and still allow the needle to reach the bulk of liquid (see Sample port in Figure 13). For the discrete sampling method, the samples pulled out of the system at different points in time can be analyzed using an appropriate technique. Discrete sampling reduces the setup complexity of the system and allows for more flexibility to extract different species and change the analytical technique to measure the concentrations.

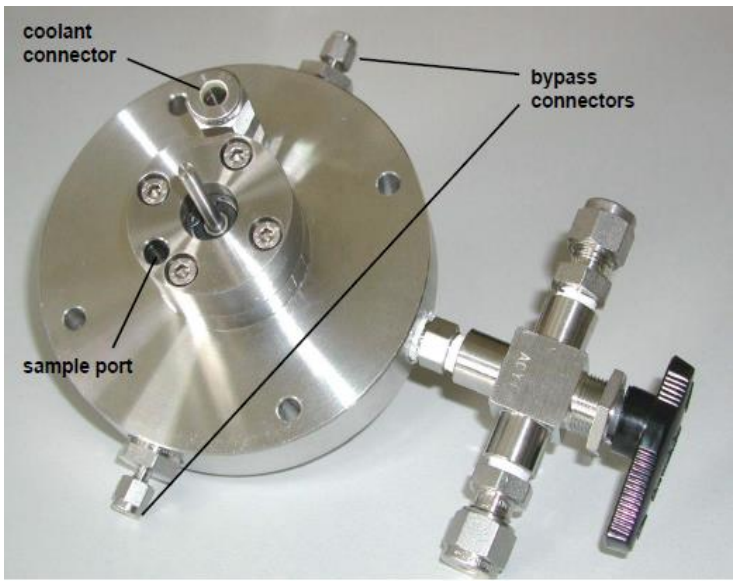

Figure 12. Upper flange of the Institut für Nukleare Entsorgungstechnik (INE) Nitsch Cell design.

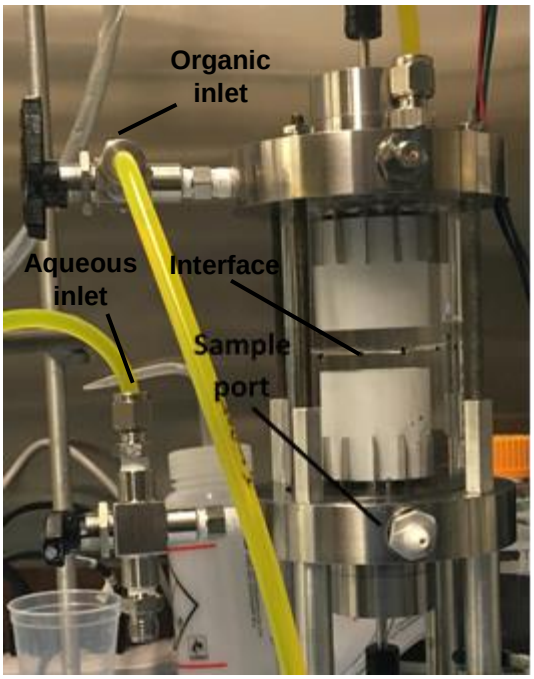

Figure 13. Interface fixed in the middle between the two guide tubes; inlet point for filling the cell; and septa blockage for the heavier phase sampling point.

- **Seals**

To check that the cell was completely sealed, a first test with water was made for several hours during which no leak was detected. However, after having used the cell filled with 0.1 M nitric acid for several days, a leak from the shaft orifice at the lower flange appeared (see Figure 14 (A)). Then, the cell was dismantled, revealing that the rubber O-rings retaining the glass cylinders and the O-ring sealing the bearing were in good condition (see Figure 14 (B) and (C)). However, the carbon seal retaining the bearing had been slightly degraded. For this reason, new seals made of Teflon, which has better resistance to strong acids, were manufactured (see Figure 14 (D)). However, even though the Teflon material extended the life of the bearing seal on the lower flange, it still had to be replaced approximately once every two weeks of using the cell daily because the shaft's continuous movement deforms it.

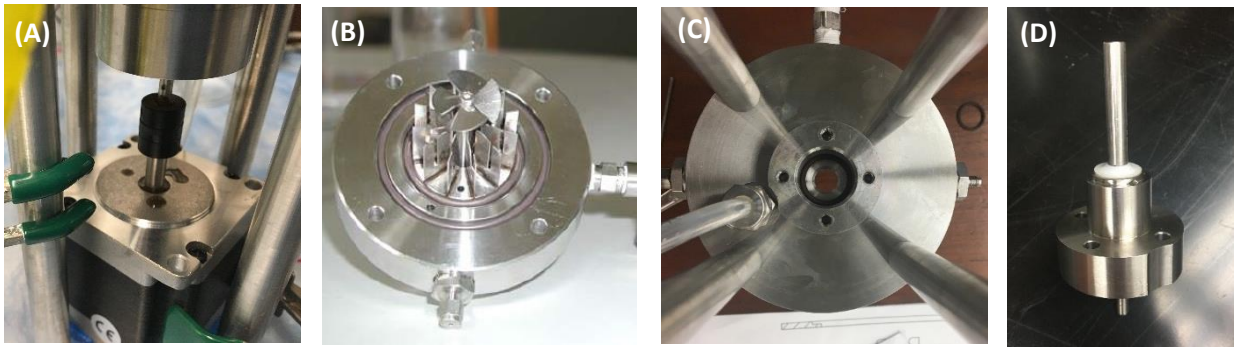

Figure 14. (A) Leak from the shaft orifice at the lower flange. (B) O-rings sealing the glass cylinders connection with the lower flange. (C) O-ring sealing the bearing unit. (D) Complete bearing unit with a Teflon seal.

- **Cleaning and Maintenance**

The first cleaning procedure that was used for the first trials with the cell was the following: after each experiment, the two phases were drained out of the cell. Afterwards, the cell was completely filled with water and the stirrers were run at high rpm for 10 minutes. Then, this procedure was repeated 2 times

with soap and afterwards, 3 more times again with distilled water. However, after facing some consistency problems with the first experiments realized in the cell, the cleaning procedure was modified.

The new cleaning method consisted of draining the cell and dismantling all the parts after each experiment. The water from the temperature bath that was in the cell at that moment was disposed of, in case it had been contaminated with the chemicals remaining in the cell during the dismantling of the parts. Then, the upper and lower flange, the stirring blades, the shafts, the glass cylinders, the guiding tubes and the inlet and sampling points were carefully cleaned individually. For this, the parts were first thoroughly rinsed with water and, afterwards, with a solution made of ethanol and 10 % volume of Nitric Acid. A brush was used to scrub all the parts once they were wet with the solution. Finally, all the parts were rinsed three more times with water and left to dry.

However, this new procedure used a stronger acid than the one used for the solvent extraction experiments (see section **Chemicals and Reagents**) and degraded the PMMA guiding tubes. For this reason, the cylinders material had to be changed to Teflon (see section **Nitsch Cell Characterization, Stirring Speed Range**), which on the one hand is not transparent but it is resistant to strong acids even during 30 days of constant exposure, according to resistance tables. [22] Even though the guiding tubes did not degrade after the experiments in this study, they should be checked regularly in case they needed to be replaced.

For the reassembly of the cell, it is important to make sure that the flow guide tubes are seated completely inside the slots of the baffles to achieve the same hydrodynamic conditions and make the experiments reproducible. In addition, after assembling the glass cylinders with the O-rings between the lower and the upper flange, it is crucial to not over-tighten the M5 bolts as a slight excess of compression may destroy the glass cylinders.

The regular maintenance required for the Nitsch cell is the replacement of the shaft seals and the shaft bearings. For the first piece, the stirrer blade has to be unscrewed, and the complete bearing unit with the O-ring and shaft seal must be removed (See Figure 14 (C) and (D)). Then, the Teflon seal has to be removed and replaced for a new one; and then all the parts have to be re-installed.

Figure 15. Shaft assembly.

For the replacement of the shaft bearings, the complete bearing unit has to be removed from the flange, and then, the circlip and the shaft assembly (see Figure 15) have to be removed from the bearing retainer. Then, the old bearing retainers have to be pulled off from the shaft and the new ones have to be placed around the shaft together with the spacer between the bearings. Finally, the shaft has to be reassembled in to the bearing retainer, and the complete bearing unit installed in the flange.

The shaft seal from the lower flange has to be replaced approximately after two weeks of continuous use of the cell. On the other hand, the lower shaft bearing has to be replaced only when the leak is not fixed just by replacing the Teflon shaft seal, which was never the case during the experiments performed in this work. Even though the same pieces from the upper flange were not affected during the experiments exposed in this study, regular checks should be done to make sure they are in good condition.

The hydrodynamics inside the cell are highly dependent on the geometry of the stirrer blades. For this reason, it is important to pay attention to them and readjust them in case they get bent. The stirrer pitch is 5 mm, and therefore, the tip-to-tip distance has to be 6 mm (5 mm pitch + 1 mm blade thickness) (see Figure 16).

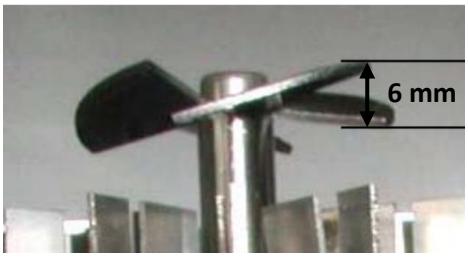

Figure 16. Correct stirrer pitch + blade thickness.

4. EXPERIMENTAL

4.1. Chemicals and Reagents

Once the Nitsch Cell and the experiment set up was robust and consistent enough, a kinetic study of the extraction of lanthanides into an organic phase containing a metal extractant was done. Previous work using a constant interfacial cell to study the extraction of different lanthanides into HEHEHP diluted in different solvents can be found; one such study is from Xianglan Wang et al., where the extraction kinetics of ytterbium (III) into HEHEHP diluted in isooctanol was investigated. [23] However, the extraction performance using acidic organophosphorus compounds can change when the extractant is added to different diluents [12] and the extraction kinetics of dysprosium (III) by 2-ethylhexylphosphonic acid mono-(2-ethylhexyl) ester (HEHEHP) diluted in Isopar L using a stirred cell has not been studied yet.

Thus, this thesis explored the kinetics of the above system. The aqueous phase consisted of dysprosium nitrate made in the lab from high purity 99.999 wt% dysprosium oxide. Dysprosium (III) (Dy^{+3}) was chosen as the metal ion to be extracted because it is one of the heavier Rare Earth Elements (REE) found in Used Nuclear Fuel and because of its high cross section for thermal neutrons (2700 barns), which makes it an easily detectable trace metal for Neutron Activation Analysis (NAA).

HEHEHEP was chosen because it is a metal extractant widely used in industry for its high selectivity of trivalent lanthanides through an ion exchange mechanism. The organic phase diluent consisted of Isopar L purchased from ExxonMobile. Isopar L was chosen as the extractant diluent because it is a broadly used solvent in industry due to its low price compared to pure diluents such as n-dodecane; its low volatility and aromatic content, and because it is odorless, compatible with most packaging materials, highly chemically stable and has low surface tension for superior surface wetting. [24]

The purpose of this preliminary study was to test the Nitsch Cell performance and to investigate the mass-transfer mechanism and provide fundamental information of the extraction system.

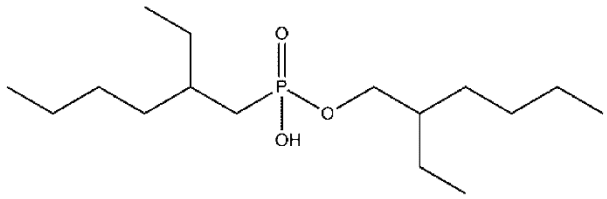

Figure 17. Schematic of a molecule of the extractant 2-ethylhexylphosphonic acid mono-(2-ethylhexyl) ester (HEHEHP).

In all the experiments throughout this study, the metal concentration in the aqueous phase used was 0.1 mM of $Dy(NO_3)_3$ in 0.1 M of HNO_3. To determine the stoichiometry of the separation reaction, extractions using different concentrations of the extractant HEHEHP diluted in Isopar L were performed: ~ 0.025 M, 0.05 M, 0.1 M and 0.2 M of HEHEHP. The kinetic studies were done for both 0.2 M and 0.05 M of HEHEHP.

4.2. Experiment procedure and setup

Experiment Procedure

The kinetics of dysprosium extraction into HEHEHEP were investigated by developing solvent extractions in the Nitsch Cell at different conditions. The procedure utilized for all of them was the following:

1. Start the water bath to let it reach the desired temperature.
2. Fill half the volume of the cell with the aqueous solvent and fill the rest with the organic phase with syringes (See section **Nitsch Cell Characterization, Filling the cell**). Weigh the syringes before and after the filling to make sure the right volume had been injected in the cell.
3. Let the phases stay in the cell for 20 minutes to exchange heat with the water bath and reach the desired temperature.
4. Set the rpm of the motors stirring each phase and wait 5 minutes to let them reach the desired rotation speed. Check that the rotation speed is correct with a handheld digital laser photo-tachometer and make sure that the mixing of each phase is not disturbing the interface.

5. Take a sample from both phases in the cell. These were analyzed afterwards to make sure the cell was cleaned before the experiment started.
6. Inject the dysprosium nitrate in the aqueous phase with a large syringe from the sampling point at the upper flange to define the start of the solvent extraction.
7. Take one sample from the aqueous phase and one from the organic phase at different time intervals (~ 10 minutes) for 1.5 h – 2 h (See section **Nitsch Cell Characterization, Sampling**).
    a. Pipette the required volume from each sample for Neutron Activation Analysis (NAA) and inject the remaining liquid back into its respective phase.
8. Stop the water bath and the motors. Drain the cell, clean it and let it dry (See section **Nitsch Cell Characterization, Cleaning and Maintenance)**.
9. Prepare the samples for NAA (See section **Analytical Method**).

Since the experiment occurred in a closed system with equal volume of the aqueous and the organic bulk, the concentration of the investigated metal in the aqueous phase ($[Dy^{+3}]^{t}_{aq}$) and the organic phase ($[Dy^{+3}]^{t}_{org}$) in any point in time should equal the initial concentration of dysprosium ($[Dy^{+3}]^{o}_{aq}$).

$$V_{aq} = V_{org} \quad \rightarrow \quad [Dy^{+3}]^{0}{}_{aq} = [Dy^{+3}]^{t}_{aq} + [Dy^{+3}]^{t}_{org} \qquad \text{Equation 3}$$

The mass balance in **Equation 3** was used to discriminate any data result of experimental errors.

The first trials to test the cell provided inconsistent data between the solvent extractions run at the same conditions. Some of the issues from the first Nitsch Cell layout exposed in section **Nitsch Cell Characterization** might have been responsible for the non-reproducibility of the experiments: the old system of motors was not capable of maintaining constant rpm throughout the experiment due to overheating of the motors and changes in liquid volume inside the cell; and the initial cleaning procedure used was not efficient enough to clean the cell properly before each new experiment. In order to improve the reproducibility of experiments, the layout of the Nitsch Cell was updated with a new system of motors

and drives to maintain constant rotation. In addition, a new and more severe cleaning procedure was used after each experiment (See section **Nitsch Cell Characterization**, **Cleaning and Maintenance)**.

Apart from these aspects, other experimental procedures were identified as potential sources of error namely the experiment start and the sampling method:

Experiment Start

Having the cell filled with the aqueous phase (0.1 mM $Dy(NO_3)_3$ in 0.1 M HNO_3) and only the solvent of the organic phase (Isopar L), the start of the solvent extraction (time = 0) was first determined by the injection of the extractant (HEHEHP) into the organic bulk. However, HEHEHP is very viscous and, in order to avoid splashes, the extractant (0.025 - 1 ml) had to be injected slowly over approximately 1-2 minutes. This very long injection could easily have a significant variability between experiments, making the initial extractant concentration distribution different between experiments and providing an undefined time zero.

For the second experiments setup, it was decided to define the start of the solvent extraction using the injection of the dysprosium in the aqueous phase in the cell, as the dysprosium nitrate has a viscosity similar to water and, therefore, can be injected more easily and quickly than the HEHEHP in the organic phase. For this, a 5.5 mM of $Dy(NO_3)_3$ in 0.1 M HNO_3 solution was prepared and 1 ml of it was injected in the aqueous phase, which initially consisted of 54 ml of 0.1 M HNO_3, with a long needle through the sampling point at the upper flange. This injection lasted approximately 10 – 20 seconds and, therefore, the time zero range was significantly reduced.

Sampling Method

The Interfacial Area / Volume ratio, as well as the interface level, have an influence on the hydrodynamics and, therefore, it is important to keep them constant for all the experiments in the kinetics study.

For the first experiments run in the Nitsch Cell, a sample of 150 μl from the aqueous and the organic phase was taken at different points in time during the experiment to track the extraction rate. In order to maintain the Interfacial Area / Volume throughout the experiment, for each sample of 150 μl that was taken from each phase, 150 μl of pure solvent was added in each phase (0.1 M of HNO_3 at the aqueous bulk and Isopar L at the organic bulk). Therefore, the bulks were slightly diluted throughout the extraction. When the slope analysis with the extracted data was done, it was realized that the extraction rate of the system was extremely slow in the Nitsch Cell, and therefore, the dilution effects could not be neglected as they were significant compared to the gradient of metal concentration versus time ($\frac{\Delta[Dy]}{\Delta t}$).

For this reason, instead of compensating the sampling volume with pure solvent, the sampling volume was reduced from 150 μl to 100 μl. In addition, only 75 μl were pipetted from the approximately 100 μl for the Neutron Activation Analysis (NAA), and the remaining sample volume was immediately injected back into its respective phase. It was noted that the interface level did not change significantly from the beginning to the end of the experiment, and the results were acceptable.

After all the changes made, the reproducibility of the second setup improved and the following experiment conditions were used for the kinetic study of dysprosium extraction into HEHEHEP:

Experiment Conditions

The solvent extractions that compose this kinetic study were all done at 20 ºC by using a water bath. To make sure that the initial temperature of the extraction was correct, the solvents of both the aqueous and organic bulks were placed in the cell with the water bath at the desired temperature for 20 min, before the experiment started. In addition, the rotation speed of the motor in the organic medium was fixed at 300 rpm, to study the effects of reducing the thickness laminar layer in the aqueous phase. For this, experiments at different rotation speeds in the range 150 rpm - 600 rpm at the aqueous bulk were developed, and each experiment was repeated two times.

In this work, the kinetics of dysprosium extraction into HEHEHEP were investigated for concentrations comparable to those used by other authors who worked with organophosphorous acids as extractants ([10],[23], [25] as outlined in section **Chemicals and Reagents**). In addition, a previous batch extraction study was done at the target concentrations and the Distribution Ratio obtained was reasonably high (see Figure 20 in section **RESULTS AND DISCUSSION**). As it is defined in section **Chemicals and Reagents**, the metal concentration in the aqueous phase was fixed at 0.1 mM for all experiments, and a kinetic study was done at both 0.2 M HEHEHEP and 0.05 M HEHEHEP in the organic phase.

4.3. Analytical Method

The concentration of dysprosium (III) in both the aqueous and organic samples taken at different points in time during the extraction was determined using Neutron Activation Analysis (NAA). NAA uses the ability of a nuclide to go to a more stable form by emitting beta or alpha particles. Each decaying unstable nuclide also emits gamma radiation with a specific energy in order to lower the energy state of the nucleus. Since each nuclide has a specific energy of gamma decay, it is possible to identify the radiation coming from the specific element of interest. In addition, the intensity of the gamma radiation is directly proportional to the number of metal ions present in a sample (see **Equation 4**, **Equation 5** and **Equation 6**) and therefore can be used as a measure of concentration. Therefore, by choosing dysprosium, which is a metal ion with high probability of capturing neutrons, the metal concentration used in the experiment can be significantly low and still be detected.

$$A_{daughter} = \emptyset\, \sigma\, N_{parent} \left(1 - e^{-\lambda\,(\text{Irradiation Time})}\right) e^{-\lambda\,(\text{Cooling Time})} \qquad \text{Equation 4}$$

$$A_{daughter} = \lambda\, N_{daughter} \qquad \text{Equation 5}$$

$$\lambda = \frac{\ln(2)}{t_{1/2}} \qquad \text{Equation 6}$$

$A_{daughter}$ being the activity of the activated nuclide, Ø the neutron flux from the nuclear reactor, σ the thermal neutron cross section of the nuclide to be activated, N_{parent} the number of atoms of the metal before the activation, $N_{daughter}$ the number of atoms of the activated nuclide, λ the decay constant of the nuclide and $t_{1/2}$ the half-life of the nuclide.

From all the natural dysprosium isotopes initially present in the sample, Dy-164 activates with a thermal neutron cross section of 2700 barns by absorbing 1 neutron and becoming Dy-165. Dy-165 is an unstable isotope that decays with a half-life of 2.33 h and emits gamma radiation with specific energy of 94.7 MeV (see Figure 18).

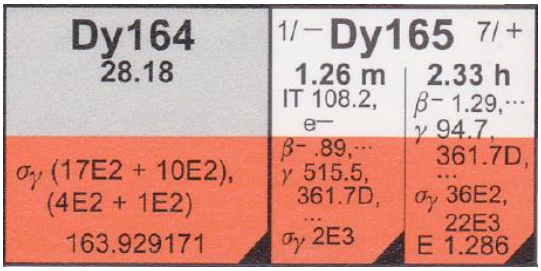

Figure 18. Data from the Chart of Nuclides of Dy-164 and Dy-165.

These analyses were performed at the UCI TRIGA Nuclear Facility, where the samples could be activated in a nuclear reactor that can provide up to 250 kW of power at steady state operation and a thermal neutron flux of $8 \cdot 10^{11}$ neutrons/cm^{2}s. Then, the samples were analyzed by gamma-ray spectroscopy using a High-Purity Germanium (HPGe) Detector. These detectors directly collect the charges produced by the ionization of the semiconductor germanium that occurs due to the gamma radiation coming from the sample. During ionization, on average, one electron-hole pair is produced for every 3 eV absorbed from the radiation, and these ions drift under an external electric field to the electrodes where they generate a pulse. These pulses are registered and converted into a spectrogram with all the gamma energies and their intensities. The concentration of metal in a sample can be calculated by comparing its energy intensity to the energy intensity of a standard sample with known concentration.

To minimize the error coming from the fluctuations in neutron flux throughout the reactor, for the experiments in this study, all the samples were placed at the same height in a spinning ring at the perimeter of the nuclear reactor, so that approximately the same flux of neutrons hit every sample.

5. RESULTS AND DISCUSSION

The extraction mechanisms and the corresponding rate laws are characteristic of each system and have to be determined by specific experiments. Experience has indicated the kinetic data give rise to laws that can be explained with simple reaction mechanisms. The extractant used in this study (HEHEHP) is an acidic extractant that performs in acidic media and therefore reacts with the metal cation in its undissociated form $(HX)_2$, where the $(HX)_2$ represents the dimer of HEHEHP. This condition, is particularly true when the extractant reacts at the interface, as the dielectric constant there is lower than the one at the bulk of the aqueous phase, reducing the extent of dissociation of the weak acid. However, if the reaction occurs in the aqueous bulk, this allows for the dissociation of the reagent (X^-), and the rate laws will be modified by taking into account either the reduced concentration of $(HX)_2$ or the fact that X^- is reacting with the metal cation.

Since HEHEHP exhibits low solubility in the aqueous phase and is a surfactant at the same time, it can be assumed that the slow step of the system occurs at the interface. This leads to the formation of an interfacial complex of the metal and the extractant, and the driving force for the transfer of this interfacial complex into the organic phase is the stronger surface activity of the reagent that replaces the less surface-active metal complex at the interface. [14] The following mechanism will be considered:

Subindex (org): organic phase; (aq): aqueous phase; (ads): adsorbed in the interface

$$\mathbf{(HX)_{2\ (org)} \rightleftarrows (HX)_{2\ (ads)}} \qquad \text{Reaction 1}$$

$$\mathbf{Dy(NO_3)_{3\ (aq)} + m(HX)_{2\ (ads)} \rightleftarrows DyX_3(HX)_{2m-3\ (ads)} + 3HNO_{3\ (aq)}} \qquad \text{Reaction 2}$$

$$\mathbf{DyX_3(HX)_{2m-3\ (ads)} \rightleftarrows DyX_3(HX)_{2m-3\ (org)}} \qquad \text{Reaction 3}$$

5.1. Defining the extraction stoichiometric coefficient

The coefficient m can be defined through equilibrium batch extractions by varying the extractant concentration. The batch extractions took place in small vials, in which equal volumes of the aqueous and organic phase were mixed together by continuous shaking of the vial for 16 minutes to ensure equilibrium was reached (other studies show that the equilibrium of Rare Earth Metals extraction into HEHEHP is achieved before 5 min [26], [27], [28]). Since the interfacial area is maximized in the vial during the shaking, the adsorbed extractant concentration can be assumed to be equal to the organic bulk concentration and, therefore, the rate-controlling reaction is:

$$\mathbf{Dy(NO_3)_{3\ (aq)} + m(HX)_{2\ (org)} \overset{k_{-1}/k_1}{\longleftrightarrow} DyX_3(HX)_{2m-3\ (org)} + 3HNO_{3\ (aq)}} \qquad \text{Reaction 4}$$

$$\mathbf{K_{eq} = \frac{k_1}{k_{-1}} = \frac{[DyX_3(HX)_{2m-3}]_{(org)}\,[H^+]_{(aq)}}{[Dy^{3+}]_{(aq)}[(HX)_2]^m_{(org)}} \frac{(\gamma_{DyX_3(HX)_{2m-3},org})(\gamma_{H^+,aq})}{(\gamma_{Dy^{3+},aq})\,(\gamma_{HM,org})} = \frac{D[H^+]^3_{(aq)}}{[(HX)_2]^m_{(org)}}} \qquad \text{Equation 7}$$

$$\mathbf{D = \frac{[DyX_3(HX)_{2m-3}]_{(org)}}{[Dy^{3+}]_{(aq)}}} \qquad \text{Equation 8}$$

The system can be assumed to be ideal since it consists of dilute solutions, and therefore, the activity coefficient ϒ can be assumed to be 1. Developing the logarithm of the left- and right-hand side of the equation and rearranging the terms, the following line is obtained:

$$\mathbf{\log K_{eq} = \log D + 3 \log [H^+] - m \log [(HX)_2]} \qquad \text{Equation 9}$$

$$\mathbf{\log D = \log K_{eq} - 3 \log [H^+] + m \log [(HX)_2]} \qquad \text{Equation 10}$$

Since the extractant concentration exists in excess in the system it can assumed to be constant throughout the extraction. Therefore, when the obtained logarithm of the equilibrium distribution ratios (log(D)) are plotted versus the logarithm of the extractant concentration (log[$(HX)_2$]), the slope of the line indicates the stoichiometric term m. Batch extractions were made with different extractant concentrations (see Figure 19) and the slope was found to be m = 2.6 (see Figure 20). Usually, the ion exchange mechanism is responsible for the extraction of rare earths using HEHEHP at low acidic range, and the transfer of a rare

earth ion is accompanied by release of three hydrogen ions from the organic phase. However, rare earth can be easily hydrolyzed, and the possible reason for which the extractant coefficient could be 2.6 is that that some hydroxide metal ions took part in the reaction ([23] [29]). However, at the acidity used in this study, 0.1 M HNO_3, is it very unlikely that there would be any hydrolyzed species. On the other hand, at a moderate acid concentration there is a chance that dysprosium is extracted with a nitrate molecule coordinated to it which would not allow for 6 HEHEHP molecules to coordinate to the metal. Hence, the non-integer coefficient experimentally obtained could be explained by a complexation reaction from 5 HEHEHP molecules from 2.5 dimers ([30]). These kind of complexes were observed using EXAFS in a recent study extracting Dy from 0.2 M HNO_3 using dibutyl-phosphoric acid complexes of $Dy(NO_3)X_2(HX)_3$ (where X is the acidic form of the extractant HDBP). [31] However, even though some other studies have reported the stoichiometric coefficient of extraction to be 2.5 ([23],[30]), the stoichiometric coefficient of trivalent lanthanides extraction with HEHEHP or other acidic organophosphorus extractants has usually been defined with m = 3 ([26], [28], [32], [33], [34], [35], [21]). Based on the literature, the reaction ratio between dysprosium and HEHEHP is probably 1 to 3, and the difference from the slope analysis can come from experimental errors.

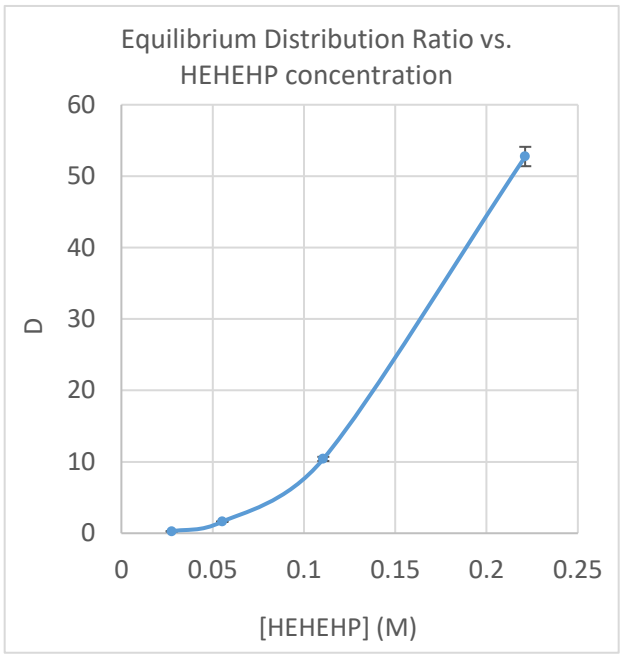

Figure 19. Equilibrium Distribution ratio for solvent extractions with different HEHEHP concentrations. $[Dy^{+3}]_{0,aq}$ = 0.1 mM; [HEHEHEP]=0.025 M, 0.05 M, 0.12 M, 0.225 M]; $[H^+]$ = 0.1 M; T = 20 ºC.

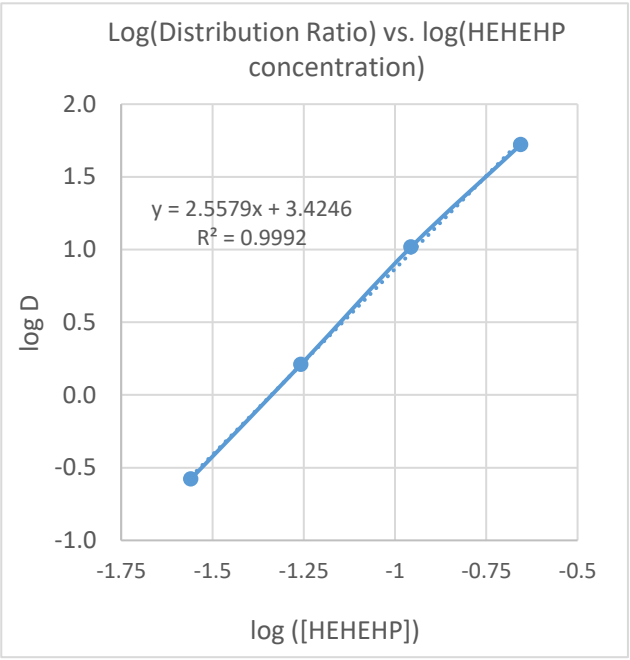

Figure 20. Logarithm of the Equilibrium Distribution Ratio versus the logarithm of the HEHEHEP concentration. $[Dy^{+3}]_{0,aq}$ = 0.1 mM; [HEHEHEP]=0.025 M, 0.05 M, 0.12 M, 0.225 M]; $[H^+]$ = 0.1 M; T = 20 ºC.

5.2. Defining the kinetic regime

Returning to the mechanism defined for the system studied in the Nitsch Cell, Reaction 2 can be assumed as the slow step of the mechanism and the reaction rate can be ilustrated from it. When defining the initial rate of the reaction it can be assumed that the backward reaction is negligible, as it has not significantly affected the system yet. Therefore, the initial rate can be defined as the forward reaction rate in **Equation 11**:

$$\mathbf{Dy(NO_3)_3}_{\ (aq)} + \mathbf{3}\ \mathbf{(HX)_2}_{\ (ads)} \overset{\mathbf{k_1}}{\underset{\mathbf{k_{-1}}}{\longleftrightarrow}} \mathbf{DyX_3(HX)_3}_{\ (ads)} + \mathbf{3HNO_3}_{\ (aq)} \qquad \text{Reaction 5}$$

$$\mathbf{r_{fwd}} = \frac{\mathbf{d}\left[\mathbf{Dy^{3+}}\right]_{(aq)}}{\mathbf{dt}} = -\mathbf{k_1}\left[\mathbf{Dy(NO_3)_3}\right]_{(aq)}\left[\mathbf{(HX)_2}\right]^{\mathbf{3}}_{\ (ads)} \qquad \text{Equation 11}$$

Solving the differential equation, the following expression is obtained:

$$\mathbf{ln}\left(\left[\mathbf{Dy^{+3}}\right]_{\mathbf{t}\ (aq)}\right) = \mathbf{ln}\left(\left[\mathbf{Dy^{+3}}\right]_{\mathbf{o}\ (aq)}\right) - \mathbf{k_1}[\mathbf{(HX)}]^{\mathbf{3}}_{\ (ads)}\,\mathbf{t} \qquad \text{Equation 12}$$

By performing an extraction and measuring the metal concentration in the aqueous phase at different points in time, the natural logarithm of the dysprosium concentration in the aqueous phase ($\ln([Dy^{+3}]_{t\ (aq)})$ versus time (t) can be plotted obtaining a line with the natural logarithm of the initial dysprosium concentration in the aqueous phase (($\ln([Dy^{+3}]_{o\ (aq)})$ as the intercept and an observed forward kinetic constant ($k_{obs} = k_1[(HX)_2]^3_{(ads)}$) as the slope (see **Equation 12**). Since the extractant concentration exist in excess in all the extractions developed in the Nitsch Cell ([HEHEHP] = 0.2 M and 0.05 M versus $[Dy(NO_3)_3]$ = 0.0001 M), the term $[(HX)_2]^3_{(ads)})]$ can be assumed to be constant.

The kinetics inside the Nitsch Cell were found to be very slow: **Table 1** shows the Distribution ratios (D) from the experiments performed, and it can be observed that the D values achieved after 1.5 h and 2.5 h of extraction are contained in a range from 2 % to 12 % of the Equilibrium Distribution ratios (D_{eq}) achieved from the batch extractions (see Figure 20). Figure 21 and Figure 23 show the liquid-liquid extractions

performed in the Nitsch Cell with 0.2 M and 0.05 M of HEHEHP respectively. It can be seen that the natural logarithm of the dysprosium concentration in the aqueous phase decreases linearly with time as in **Equation 12**, which corroborates that the backward reaction is not significant for the first 1.5 – 2.5 h of the experiment and, therefore, the initial reaction can indeed be defined as in **Equation 11**.

Table 1. Distribution ratios of the dysprosium (III) extraction into HEHEHP from equilibrium batch extractions and from extractions in the Nitsch Cell, stirring the organic phase at 300 rpm and the aqueous phase at different stirring speeds. Equilibrium batch extractions duration = 16 min; Nitsch Cell extractions duration = 1.5 h (extraction into 0.05 M of HEHEHP) and 2.5 h (extraction into 0.2 M of HEHEHP); $[Dy^{+3}]_{0,aq}$ = 0.1 mM; [HEHEHP] = 0.2 M and 0.05 M; $[H^{+}]$ = 0.1 M; T = 20 ºC.

Equilibrium Batch Extractions		**Nitsch Cell extraction into 0.05 M of HEHEHP**			**Nitsch Cell extraction into 0.2 M of HEHEHP**		
HEHEHP (M)	**$D_{eq} \pm \sigma_{dev}$**	**Aq. Stirring Speed (rpm)**	**$D \pm \sigma_{dev}$**	**% of D_{eq}**	**Aq. Stirring Speed (rpm)**	**$D \pm \sigma_{dev}$**	**% of D_{eq}**
0.05	1.623 ± 0.029	150	0.040 ± 0.038	2.46	150	0.917 ± 0.296	2.04
0.2	45.000 ± 2.710	225	0.050 ± 0.013	3.08	-	-	-
		300	0.058 ± 0.004	3.57	300	1.443 ± 0.132	3.21
		400	0.055 ± 0.004	3.39	400	2.144 ± 0.503	4.76
		500	0.096 ± 0.051	5.91	600	5.330 ± 0.900	11.84

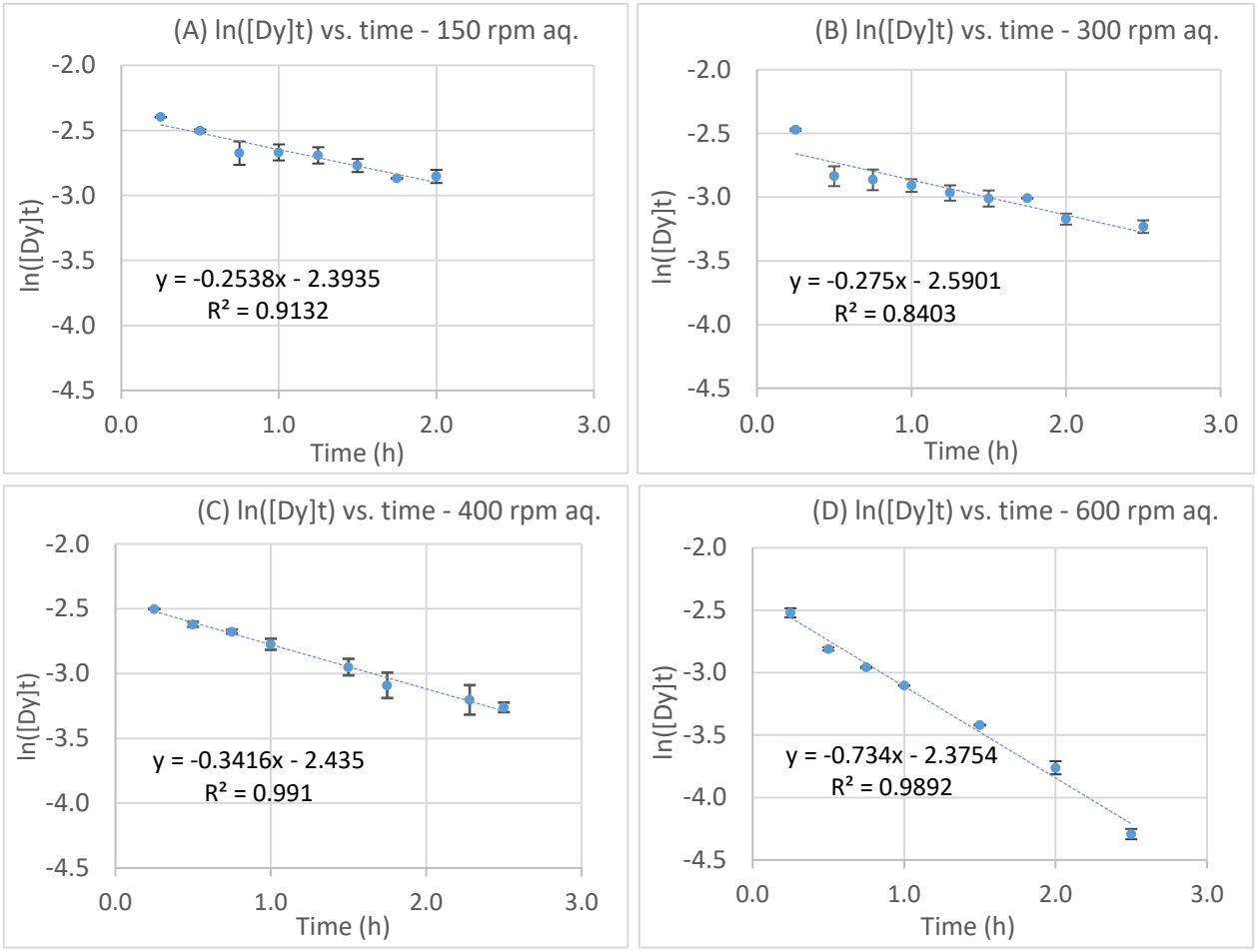

Figure 21. Natural logarithm of dysprosium concentration of the aqueous phase at different points in time for different stirring speeds in the aqueous phase: (A) 150 rpm; (B) 300 rpm; (C) 400 rpm and (D) 600 rpm. $[Dy^{+3}]_{0,\,aq}$ = 0.1 mM; [HEHEHEP]=0.2 M; $[H^+]$ = 0.1 M; T = 20 ºC; Organic phase stirring speed = 300 rpm.

The observed initial kinetic constants obtained from the graphs in Figure 21 are plotted versus the stirring speed in the aqueous phase of each experiment in Figure 22. No extractions were done above 600 rpm because the interface broke at such high rpm, resulting in the mixture of the two phases. Even though small undulations appeared at the interface at 600 rpm, this hydrodynamic condition was studied because the contact area was still stable. However, the significant increase of the K_{obs} from 400 rpm to 600 rpm indicates that the extraction rate might not only be attributed to the decrease of the aqueous stagnant layer of the interface, but also to an increase in interfacial area generated by the undulations. For this

reason, the stirring speed range with constant interfacial area is considered only from 0 to 400 rpm, and the last point in Figure 22 this is discriminated.

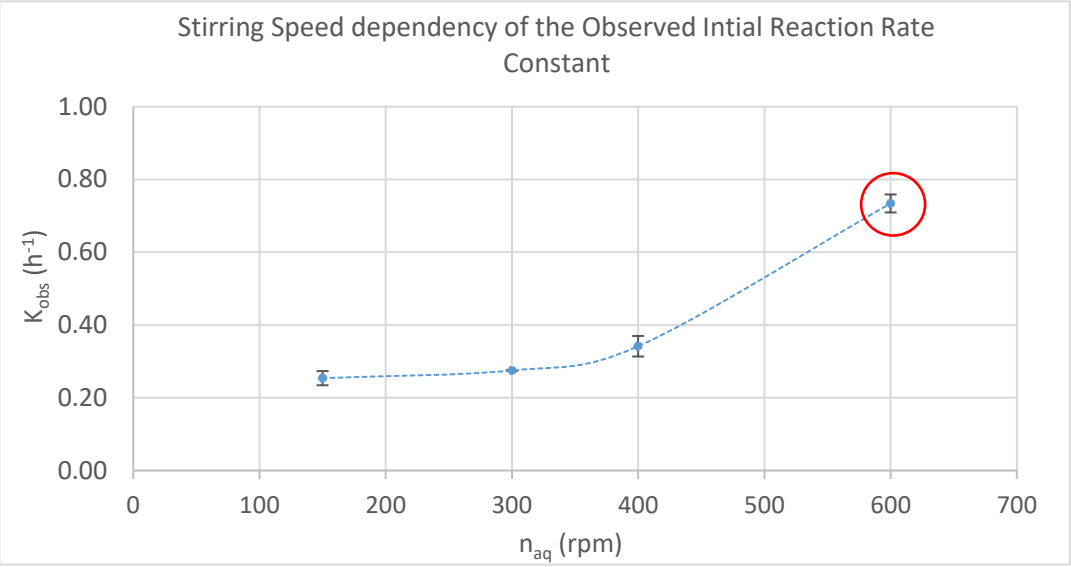

Figure 22. Stirring Speed dependency of the Observed Initial Reaction Rate Constant. $[Dy^{+3}]_{0,\,aq}$ = 0.1 mM; [HEHEHP] = 0.2 M; $[H^{+}]$ = 0.1 M; T = 20 ºC; Organic phase stirring speed = 300 rpm; Aqueous phase stirring speed = 150 - 600 rpm.

The increase in extraction rate with the aqueous stirring speed that can be observed in Figure 22 indicates that the chemical reaction occurring at the interface is not slow enough to be competitive with the mass transfer rate. Therefore, it can be concluded that the extraction rate is diffusion controlled, and the kinetics occur in a diffusion-limited regime for stirring speeds of 150 rpm to 400 rpm.

Dong *et al.* also defined the kinetic regime as diffusion-limited for the extraction of 0.2 M of lutetium(III) into 0.3 M of HEHEHEP diluted in hydrochloric medium. However, the stirred cell design used only allowed them to study the kinetics for stirring speeds up to 180 rpm. The kinetics study that Wang *et al.* developed for the extraction of 0.03 M of ytterbium (III) into 0.3 M of HEHEHEP diluted in isooctanol also showed an increasing linear relationship between the observed extraction rate and the aqueous stirring speed from 150 to 400 rpm. As with the Nitsch Cell, the design of their cell did not allow them to study higher mixing speeds without disturbing the interface. [23]

As already known for some systems, the extraction regime can be altered from limitation by diffusion to limitation by chemical reaction through the reduction of the extractant concentration. [36] For this reason, experiments with a concentration 4 times lower were performed (See Figure 23). Decreasing the extractant concentration 4 times resulted in a shift of the observed kinetic constants to values approximately 10 times smaller. Figure 24 shows a linear increase of the observed initial extraction rate with aqueous stirring speeds from 150 rpm to 500 rpm, which would indicate that the extraction regime is still diffusion-limited. However, the high standard deviation observed for the experiments at 500 rpm in Figure 24 might indicate that the undulations of the interface are not negligible. If that point is disregarded, a plateau region seems to begin from 400 rpm on, which would indicate that the heterogeneous chemical reaction is becoming competitive with the diffusion of dysprosium in the aqueous phase. However, this could not be further confirmed because of the disturbances at the interface that appeared at higher stirring speeds.

For future studies, a new geometry of the Nitsch Cell with a smaller diameter and equal interfacial area and volume ratio could be built to try to reach stirring speeds higher than 400 rpm. However, future work could also focus on using the same Nitsch Cell design to potentially reach the chemical-limited regime by studying the system at lower temperatures. Changes in temperature should not greatly influence the flux as, according to Einstein-Stokes equation (see **Equation 13**), the diffusion coefficient of particles in a fluid median depends linearly on temperature, whereas the dependence of a chemical reaction on temperature is exponential, according to the Arrhenius equation (see **Equation 14**). Therefore, decreasing the temperature in which the extraction occurs will decrease the chemical reaction rate making it relatively more competitive with the diffusion rate. This would potentially neglect the dependency of the extraction rate on the stirring speed, allowing a plateau region to appear when plotting the observed extraction rate versus the stirring speed.

$$\mathbf{Dif} = \frac{\mathbf{k_B\ T}}{\mathbf{6\pi r\mu}}$$ Equation 13

Dif: diffusion constant; k_B: Boltzmann's constant; T: temperature; r: radius of the particle; μ: viscosity of the medium

$$\mathbf{K = A\ e^{-\frac{Ea}{RT}}}$$ Equation 14

K: forward rate constant; A: pre/exponential factor; Ea: activation energy; R: universal gas constant; T: temperature

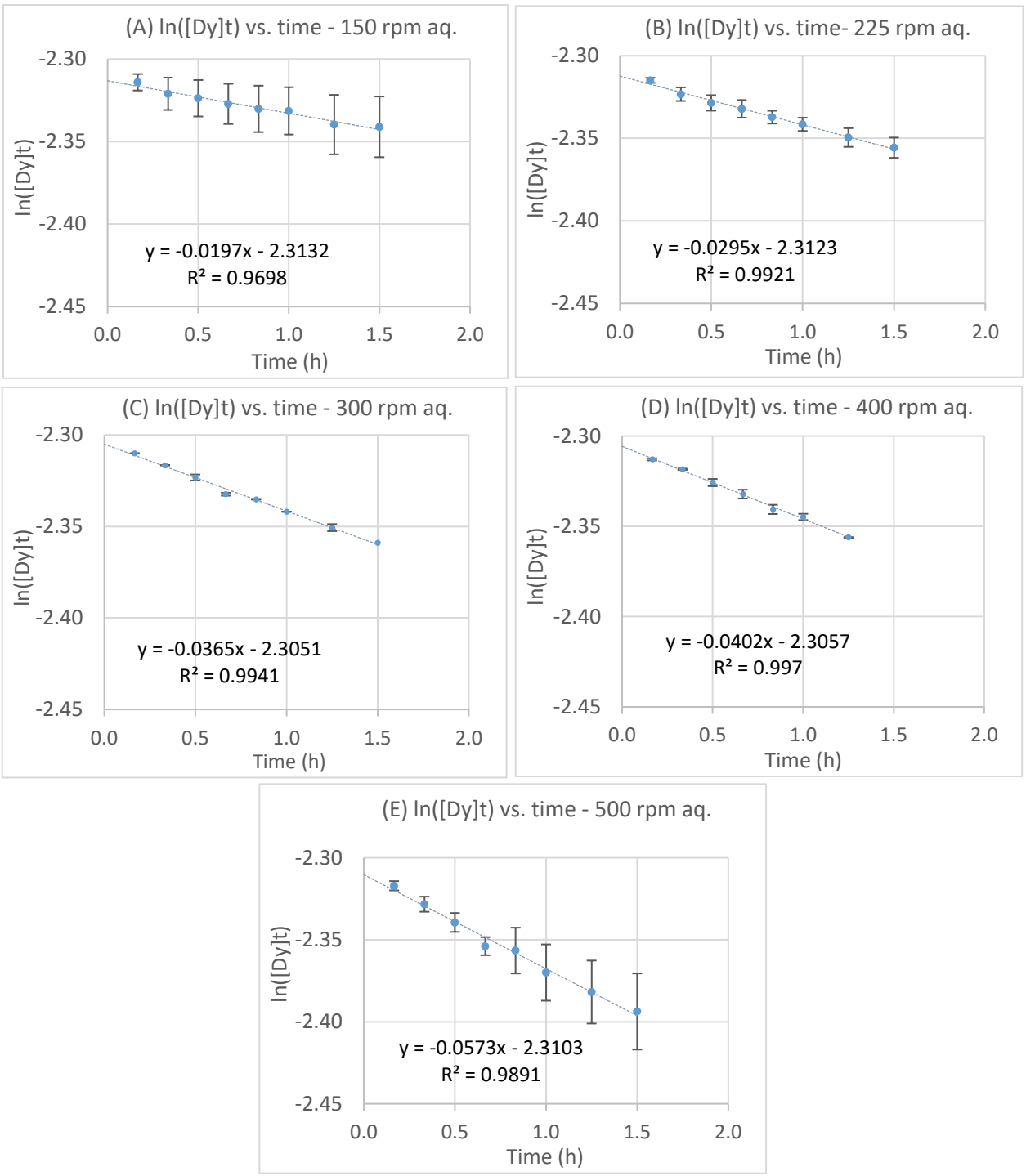

Figure 23. Natural logarithm of dysprosium concentration of the aqueous phase at different points in time for different stirring speeds in the aqueous phase: (A) 150 rpm; (B) 225 rpm; (C) 300 rpm; (D) 400 rpm and (E) 500 rpm. $[Dy^{+3}]_{0,aq}$ = 0.1 mM; [HEHEHEP]=0.05 M; $[H^+]$ = 0.1 M; T = 20 ºC; Organic phase stirring speed = 300 rpm.

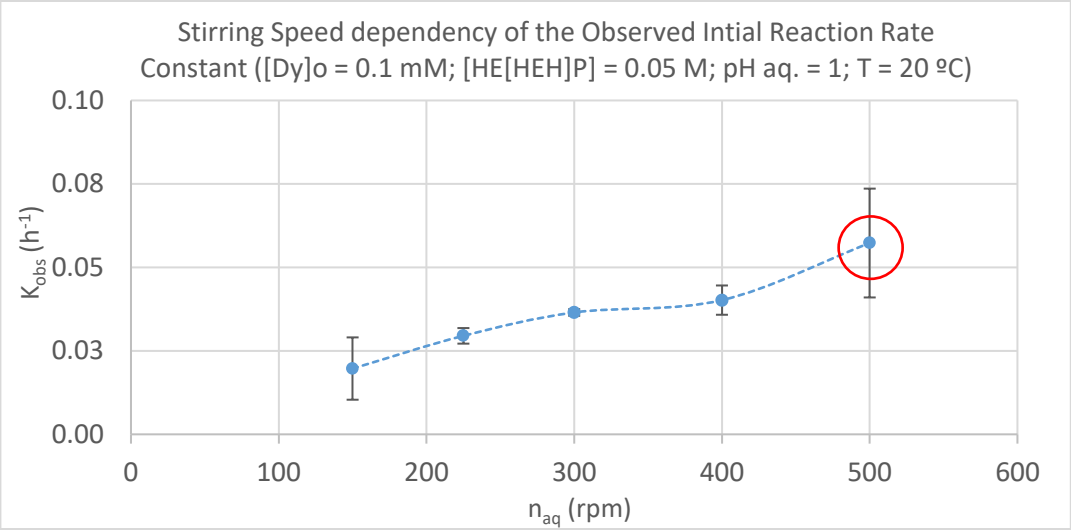

Figure 24. Stirring Speed dependency of the Observed Initial Reaction Rate Constant. $[Dy^{+3}]_{0,aq}$ = 0.1 mM; [HEHEHP] = 0.05 M; $[H^+]$ = 0.1 M; T = 20 ºC; Organic phase stirring speed = 300 rpm; Aqueous phase stirring speed = 150 - 500 rpm.

5.3. Defining Individual Mass Transfer Coefficients

The flux of dysprosium (j_{Dy}^{+3}) in the stirred cell can be calculated according to the decrease in metal concentration ($\Delta[Dy^{+3}]$) during a small-time gradient (Δt), the interfacial area (A) and the cell volume (V), as shown in **Equation 15**:

$$\mathbf{j_{Dy^{+3}}} = \left| \frac{\mathbf{\Delta[Dy^{+3}]V}}{\mathbf{\Delta t\, A}} \right| \qquad \text{Equation 15}$$

The following plots illustrate the dysprosium flux during the first 1.5 h of the solvent extractions performed in the Nitsch Cell, and its dependence on the stirring speed of the aqueous phase for two different concentrations of extractant in the organic phase (see Figure 25 and Figure 26):

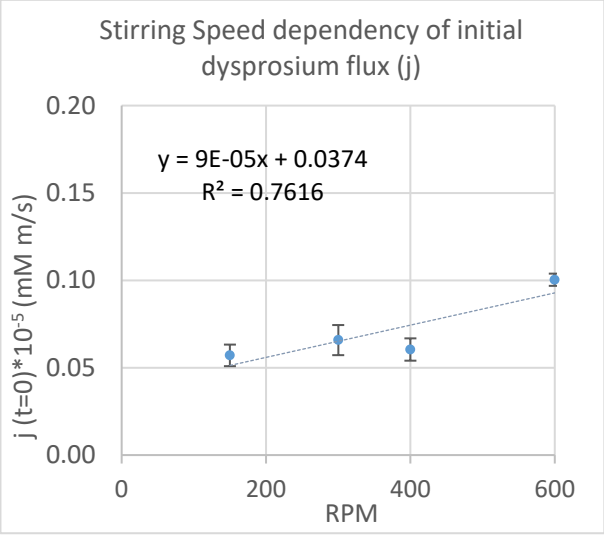

Figure 25. Stirring Speed dependency of initial dysprosium flux. $[Dy^{+3}]_{0,\,aq}$ = 0.1 mM; [HEHEHP] = 0.2 M; $[H^{+}]$ = 0.1 M; T = 20 ºC; Organic phase stirring speed = 300 rpm; Aqueous phase stirring speed = 150 - 500 rpm.

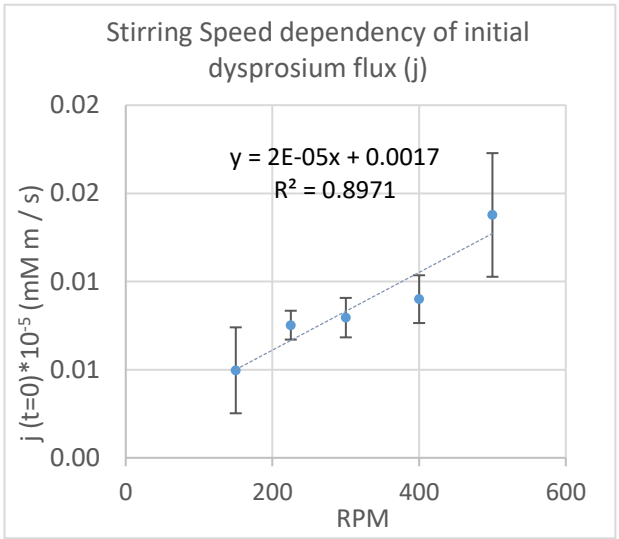

Figure 26. Stirring Speed dependency of initial dysprosium flux. $[Dy^{+3}]_{0,\,aq}$ = 0.1 mM; [HEHEHP] = 0.05 M; $[H^{+}]$ = 0.1 M; T = 20 ºC; Organic phase stirring speed = 300 rpm; Aqueous phase stirring speed = 150 - 600 rpm.

As mentioned in the previous section, the interfaces generated at 500 rpm and 600 rpm aqueous stirring speeds were stable but undulated, and the consequential increase of interfacial area was most likely

responsible for the significant increase of the metal flux observed. For this reason, only the fluxes from the experiments between 150 rpm and 400 rpm are considered in Figure 27:

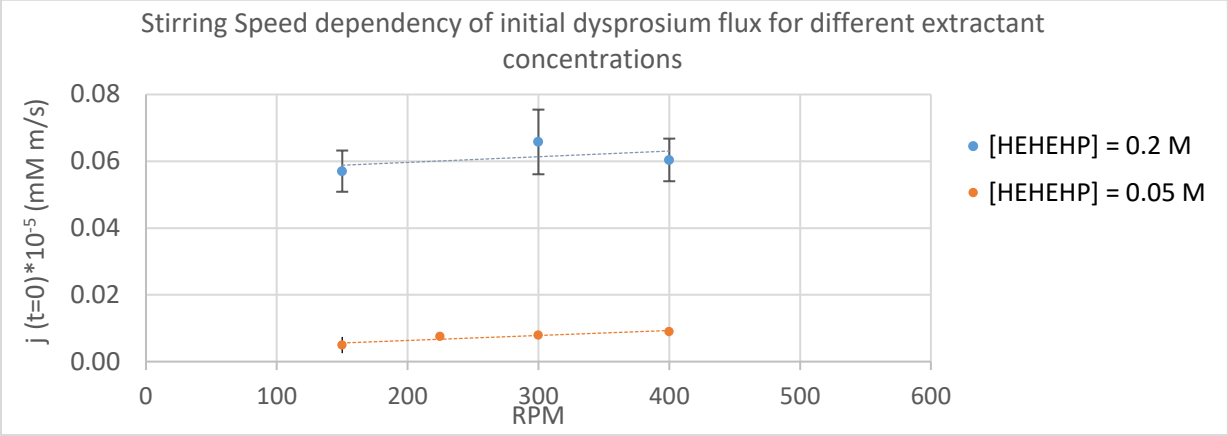

Figure 27. Stirring Speed dependency of initial dysprosium flux for different extractant concentrations. $[Dy^{+3}]_{0,aq}$ = 0.1 mM; [HEHEHP] = 0.2 M and 0.05 M; $[H^{+}]$ = 0.1 M; T = 20 ºC; Organic phase stirring speed = 300 rpm; Aqueous phase stirring speed = 150 - 400 rpm.

The metal flux has a first order dependence on metal concentration and the diffusion of dysprosium ions is the limiting step, as the mass transfer resistance is located in the aqueous phase. [25] The flux of dysprosium (j_{Dy}^{+3}) depends on the individual mass transfer coefficient (k_{Dy}^{+3}) and the gradient between the bulk concentration of metal ($[Dy^{+3}]$) and the concentration at the interface ($[Dy^{+3}]^{*}$):

$$\mathbf{j_{Dy^{+3}} = k_{Dy^{+3}}([Dy^{+3}] - [Dy^{+3}]^{*})} \qquad \text{Equation 16}$$

As it has been concluded previously, the extraction rate is limited by diffusion of dysprosium ions for the aqueous stirring speed range 150 rpm – 400 rpm. Therefore, since the reaction rate can be considered very fast compared to the diffusion rate at these hydrodynamic conditions, the dysprosium concentration at the interface can be neglected. Therefore, the individual mass transfer coefficients can be found by dividing the initial metal flux by the initial metal concentration (see **Table 2** and **Table 3**):

Table 2. Individual Mass Transfer Coefficients of 0.1 mM of dysprosium (III) extraction into 0.2 M of HEHEHP for different stirring speeds in the aqueous phase. $[Dy^{+3}]_{0,\,aq}$ = 0.1 mM; [HEHEHP] = 0.2 M; $[H^{+}]$ = 0.1 M; T = 20 ºC; Organic phase stirring speed = 300 rpm; Aqueous phase stirring speed = 150 - 400 rpm.

Aqueous Stirring Speed (rpm)	Mass Transfer Coefficient (m/s)
150	$5{,}70 \cdot 10^{-6}$
300	$6{,}58 \cdot 10^{-6}$
400	$6{,}04 \cdot 10^{-6}$

Table 3. Individual Mass Transfer Coefficients of 0.1 mM of dysprosium (III) extraction into 0.05 M of HEHEHP for different stirring speeds in the aqueous phase. $[Dy^{+3}]_{0,\,aq}$ = 0.1 mM; [HEHEHP] = 0.05 M; $[H^{+}]$ = 0.1 M; T = 20 ºC; Organic phase stirring speed = 300 rpm; Aqueous phase stirring speed = 150 - 400 rpm.

Aqueous Stirring Speed (rpm)	Mass Transfer Coefficient (m/s)
150	$4{,}96 \cdot 10^{-8}$
225	$7{,}52 \cdot 10^{-8}$
300	$7{,}95 \cdot 10^{-8}$
400	$9{,}00 \cdot 10^{-8}$

6. CONCLUSIONS

The effect of interfacial area in a given system is the parameter usually studied to differentiate between chemical reaction taking place in the bulk phase or at the interface. When defining the reaction mechanism for the system studied in this work (see **Reaction 1**, **Reaction 2**, **Reaction 3** and **Equation 11**) it was assumed that the rate controlling reaction occurred at the interface instead of in the bulk because of the acidic and surfactant characteristics of the extractant. The experiments performed confirmed this hypothesis as the extraction rate was not independent of the interfacial area: the extraction rate increased significantly with the increase in contact area, which occurred when undulations at the interface appeared due to high stirring speeds. In addition, the equilibrium batch extractions performed indicated that the extraction stoichiometric coefficients are 1 and 2.6 for Dy^{+3} and HEHEHP, respectively. Even though some other studies have shown extractant stoichiometric coefficients of 2.5, justifying that hydrolyzed lanthanide ions are produced in the reaction or that 5 molecules of HEHEHEP from 2.5 dimers contribute to the reaction ([23],[30], [31]), the majority of studies of the extraction of trivalent lanthanides into HEHEHP or other acidic organophosphorus extractants show a stoichiometric coefficient of 3 ([26], [28], [32], [33], [34]). Based on that, the reaction ratio between dysprosium and HEHEHP is probably 1 to 3, and the difference from the slope analysis can come from experimental errors.

The kinetics inside the Nitsch Cell were found to be very slow, as the distribution ratios achieved for the experiments after 2.5 h were less than the 10 % of the equilibrium distributions ratios. In addition, since the natural logarithm of the dysprosium concentration in the aqueous phase decreased linearly with time during all the time range studied, it was confirmed that the backward reaction from the equilibrium expression in **Reaction 5** had not significantly affected the system yet. Therefore, the initial extraction rate alone in **Equation 11** was assumed to be sufficient to define the system.

The observed initial kinetic constants obtained from the solvent extractions into 0.2 M of HEHEHP showed an increasing tendency with the increase of the aqueous stirring speed from 150 rpm to 400 rpm. This indicated that the kinetic regime was diffusion-limited, as was also concluded in the study that Wang et *al.* developed for the extraction of 0.3 M of ytterbium (III) into 0.3 M of HEHEHEP diluted in isooctanol at the same aqueous stirring speeds. [23] Decreasing the extractant concentration 4 times resulted in a shift of the observed kinetic constants to values approximately 10 times smaller. Even though the extraction rate was also mainly controlled by the diffusion rate from 150 rpm to 400 rpm of aqueous stirring speeds, indicating a diffusion-limited regime, the regime at higher rpm should be further analyzed. The start of the plateau region seemed to appear at 400 rpm, but the start of the reaction-limited regime from this stirring speed could not be further confirmed because the experiments done at higher rpm showed significant undulations at the interface, increasing the interfacial area and making the observed initial kinetic constant increase and leave the plateau zone.

To try to reach a reaction-limited regime for the extraction system studied, a new geometry of the Nitsch Cell with smaller diameter and equal interfacial area and volume ratio could be built to try to reach stirring speeds higher than 400 rpm. Future work could also focus on using the same Nitsch Cell design to potentially reach the chemical-limited regime by studying the system at lower temperatures, as this would make the chemical reaction rate more competitive with the diffusion rate, according to the Einstein-Stokes equation and the Arrhenius equation (see **Equation 13** and **Equation 14**). Nevertheless, the fact that the extraction rate was diffusion-limited for the range studied indicates a fast chemical reaction. This is desirable from a technological point of view as it allows short contacting times in an extractor. In addition, this indicates that the extraction mixing speed is a parameter that can be optimized to minimize the mixing energy required and still achieve the desired performance of an extraction process. Moreover, the fact that the chemical reaction is very fast indicates that the dysprosium reacts almost immediately after diffusing through the aqueous laminar layer and reaching the interface. Consequently, the initial

dysprosium fluxes of each experiment and their dependency on the stirring speed could be analyzed and the individual mass transfer coefficients for each hydrodynamic condition could be provided.

The kinetic information from solvent extraction systems is a crucial aspect for enabling further advancements in design and operation of future units for nuclear energy generation. The Nitsch Cell built in this project is a piece of equipment that will enable the Nuclear Group at UCI to develop further kinetic studies for reprocessing spent nuclear fuel and reducing the radioactive waste generated in nuclear plants in a more efficient, safe, sustainable and economic manner. This will determine the success of future advanced nuclear fuel reprocessing facilities and will position nuclear power as a powerful solution for the global energy crisis that we will prospectively experience in the near future.

REFERENCES

[1] U.S. Energy Information Administration, “International Energy Outlook 2017 Overview,” *Int. Energy Outlook*, vol. IEO2017, no. September 14, 2017.

[2] B. E. Layton, “A comparison of energy densities of prevalent energy sources in units of joules per cubic meter,” *Int. J. Green Energy*, vol. 5, no. 6, pp. 438–455, 2008.

[3] D. L. Davidson, “The Role of Computational Fluid Dynamics in Process Industries,” *Bridg.*, vol. 32, no. 4, pp. 9–15, 2002.

[4] K. E. Wardle, “Liquid-Liquid Mixing Studies in Annular Centrifugal Contactors Comparing Stationary Mixing Vane Options,” *Solvent Extr. Ion Exch.*, vol. 33, no. 7, pp. 671–690, 2015.

[5] T. A. Todd, “Solvent Extraction Research and Development in the U . S . Fuel Cycle Program,” *Int. Solvent Extr. Conf.*, p. INL/CON-11-20934, 2011.

[6] K. Binnemans *et al.*, “Recycling of rare earths: A critical review,” *J. Clean. Prod.*, vol. 51, pp. 1–22, 2013.

[7] T. Babikian and M. Nilsson, “Extraction Kinetics and Hydrodynamics in Miniature Annular Centrifugal Contactors,” *Proc. from Glob. 2017, Seoul, Korea*, pp. 1–52, 2017.

[8] K. E. Wardle, T. R. Allen, and R. Swaney, “Computational fluid dynamics (CFD) study of the flow in an annular centrifugal contactor,” *Sep. Sci. Technol.*, vol. 41, no. 10, pp. 2225–2244, 2006.

[9] G. R. Choppin, “Solvent Exraction Principles and Practice,” *Solvent Extr. Princ. Pract.*, vol. Second Edt, pp. 1–252, 2004.

[10] N. E. El-hefny, “Kinetics and mechanism of extraction and stripping of neodymium using a Lewis cell,” vol. 46, pp. 623–629, 2007.

[11] H. Reinhardt, “Liquid-liquid extraction equipment,” *Hydrometallurgy*, vol. 42, p. 441, 1996.

[12] C. N. Separation, D. Effect, O. Extractant, and H. M. Loading, “THE EFFECT OF DILUENT IN THE LIQUID-LIQUID EXTRACTION OF COBALT AND NICKEL USING ACIDIC ORGANOPHOSPHORUS COMPOUNDS A typical example of category (a) is the extraction,” 1978.

[13] J. T. J. Colven, “Equipment for Nuclear Fuel Reprocessing,” *Sep. Eng. Div.*, no. October, 1957.

[14] P. R. Danesi, R. Chiarizia, C. F. Coleman, and P. R. Danesi, “The Kinetics of Metal Solvent Extraction,” vol. 8980, no. May, 2017.

[15] A. Szent-gyorgyi, “Diffusion and Reaction 12,” pp. 813–866, 2008.

[16] C. V. Sternling and L. E. Scriven, “Interfacial turbulence: Hydrodynamic instability and the marangoni effect,” *AIChE J.*, vol. 5, no. 4, pp. 514–523, 1959.

[17] P. R. Danesi, C. Cianetti, E. P. Horwitz, and H. Diamond, “Armollex: An Apparatus For Solvent Extraction Kinetic Measurements,” *Sep. Sci. Technol.*, vol. 17, no. 7, pp. 961–968, 1982.

[18] X. Yang, X. Wang, C. Wei, S. Zheng, Q. Sun, and D. Wang, “Hydrometallurgy Extraction kinetics of tantalum by MIBK from pulp using Lewis cell,” *Hydrometallurgy*, vol. 131–132, pp. 34–39, 2013.

[19] J. Niemczewska, R. Cierpiszewski, and J. Szymanowski, “Mass transfer of zinc(II) extraction from hydrochloric acid solution in the Lewis cell,” *Desalination*, vol. 162, no. 1–3, pp. 169–177, 2004.

[20] D. B. Dreisinger and W. C. Cooper, “THE DIFFUSION COEFFICIENT OF HEHEHP IN HEPTANE MEASURED BY THE MODIFIED STOKES CELL TECHNIQUE AT TEMPERATURES BETWEEN 25,” vol. 6299, no. June 2017, 2007.

[21] J. Dong, Y. Xu, L. Wang, X. Huang, Z. Long, and S. Wu, “Thermodynamics and kinetics of lutetium extraction with HEH(EHP) in hydrochloric acid medium,” *J. Rare Earths*, vol. 34, no. 3, pp. 300–307,

2016.

[22] Thermo Fisher Scientific, “Chemical Compatibility Guide: Effects of chemicals on plastics,” 2016.

[23] X. Wang, S. Meng, and D. Li, “Extraction kinetics of ytterbium (III) by 2-ethylhexylphosphonic acid mono- (2-ethylhexyl) ester in the presence of isooctanol using a constant interfacial cell with laminar flow,” vol. 71, pp. 50–55, 2010.

[24] “Foxboro Rev Date : August 2008 Product Name : ISOPAR M FLUID Product Code :,” pp. 1–10, 2008.

[25] F. KneißI, A. Geist, and W. Nitsch, “Europium Extraction Into D2EHPA: Kinetics of Mass Transfer in a Stirred Cell,” *Solvent Extr. Ion Exch.*, vol. 17, no. 3, pp. 475–493, 1999.

[26] M. Labanca, W. Scal, and F. E. Á. Láctico, “DIDYMIUM SEPARATION FROM LANTHANUM BY SOLVENT EXTRACTION USING 2-ETHYLHEXYLPHOSPHONIC ACID MONO-2-ETHYLHEXYL ESTER AND LACTIC ACID SOLVENTES USANDO ÉSTER MONO-2-ETIL-HEXÍLICO DO ÁCIDO,” pp. 373–380, 2016.

[27] V. E. Holfeltz *et al.*, “Effect of HEH[EHP] impurities on the ALSEP solvent extraction process,” *Solvent Extr. Ion Exch.*, vol. 36, no. 1, pp. 1–19, 2017.

[28] X. Huang, J. Dong, L. Wang, Z. Feng, Q. Xue, and X. Meng, “Selective recovery of rare earth elements from ion-adsorption rare earth element ores by stepwise extraction with HEH(EHP) and HDEHP,” *Green Chem.*, vol. 19, no. 5, pp. 1345–1352, 2017.

[29] D. Wu, C. Niu, D. Li, and Y. Bai, “Solvent extraction of scandium(III), yttrium(III), lanthanum(III) and gadolinium(III) using Cyanex 302 in heptane from hydrochloric acid solutions,” *J. Alloys Compd.*, vol. 374, no. 1–2, pp. 442–446, 2004.

[30] G. W. Mason, D. N. Metta, D. F. Peppard, and C. Division, “THE EXTRACTION OF SELECTED M(III) METALS BY BIS 2-ETHYLHEXYL PHOSPHORIC ACID IN n-HEPTANE,” vol. 38, no. Iii, pp. 2077–2079, 1976.

[31] A. D. Braatz, M. R. Antonio, and M. Nilsson, “Structural study of complexes formed by acidic and neutral organophosphorus reagents,” *Dalt. Trans.*, vol. 46, no. 4, pp. 1194–1206, 2017.

[32] D. F. Peppard, G. W. Mason, and G. Giffint, “EXTRACTION OF SELECTED TRIVALENT LANTHANIDE AND ACTINIDE CATIONS BY BIS (HEXOXY-ETHYL) PHOSPHORIC ACID * A WIDE variety of mono-acidic phosphorus-based extractants , (X)(Y) PO (OH), in a carrier diluent have been reported as extractants of metalli,” vol. 27, no. 1957, pp. 1683–1691, 1965.

[33] Z. Kolařík and H. Pánková, “Acidic organophosphorus extractants-I Extraction of lanthanides by means of dialkyl phosphoric acids-effect of structure and size of alkyl group,” *J. Inorg. Nucl. Chem.*, vol. 28, no. 10, pp. 2325–2333, 1966.

[34] A. T. Kandil and K. Farah, “THERMODYNAMIC STUDIES OF TOPO ADDUCTS OF EUROPIUM AND TERBIUM TRIS-TTA CHELATES,” vol. 42, pp. 1491–1494, 1979.

[35] C. R. Adhikari, H. Narita, and M. Tanaka, “Solvent extraction equilibrium of dysprosium(III) from nitrate solutions with 2-ethylhexylphosphonic acid mono-2-ethylhexyl ester,” *Ind. Eng. Chem. Res.*, vol. 51, no. 50, pp. 16433–16437, 2012.

[36] W. Nitsch and B. Kruis, “The influence of flow and concentration on the mass transfer mechanism in chelating liquid/liquid-extractions,” *J. Inorg. Nucl. Chem.*, vol. 40, no. 5, pp. 857–864, 1978.